

QCD AND LIGHT-FRONT HOLOGRAPHY*

STANLEY J. BRODSKY†

SLAC National Accelerator Laboratory
Stanford University, Stanford, CA 94309, USA
and

CP³-Origins, Southern Denmark University, Odense, Denmark

GUY F. DE TÉRAMOND‡

Universidad de Costa Rica, San José, Costa Rica

(Received October 13, 2010)

The soft-wall AdS/QCD model, modified by a positive-sign dilaton metric, leads to a remarkable one-parameter description of nonperturbative hadron dynamics. The model predicts a zero-mass pion for zero-mass quarks and a Regge spectrum of linear trajectories with the same slope in the leading orbital angular momentum L of hadrons and the radial quantum number N . Light-front holography maps the amplitudes which are functions of the fifth dimension variable z of Anti-de Sitter space to a corresponding hadron theory quantized on the light front. The resulting Lorentz-invariant relativistic light-front wave equations are functions of an invariant impact variable ζ which measures the separation of the quark and gluonic constituents within the hadron at equal light-front time. The result is to a semiclassical frame-independent first approximation to the spectra and light-front wavefunctions of meson and baryon light-quark bound states, which in turn predict the behavior of the pion and nucleon form factors. The theory implements chiral symmetry in a novel way: the effects of chiral symmetry breaking increase as one goes toward large interquark separation, consistent with spectroscopic data, and the hadron eigenstates generally have components with different orbital angular momentum; *e.g.*, the proton eigenstate in AdS/QCD with massless quarks has $L = 0$ and $L = 1$ light-front Fock components with equal probability. The soft-wall model also predicts the form of the non-perturbative effective coupling $\alpha_s^{\text{AdS}}(Q)$ and its β -function which agrees with the effective coupling α_{g_1} extracted from the Bjorken sum rule. The AdS/QCD model can be systematically improved by using its complete orthonormal solutions to diagonalize the full QCD light-front Hamiltonian or by applying the Lippmann-Schwinger method in order to systematically include the QCD interaction terms. A new perspective on quark and gluon condensates is also reviewed.

PACS numbers: 11.10.Kk, 11.25.Sq, 11.25.Tq, 12.38.Aw

* Lecture presented by S.J. Brodsky at the L Cracow School of Theoretical Physics “Particle Physics at the Dawn of the LHC”, Zakopane, Poland, June 9–19, 2010.

† sjbth@slac.stanford.edu

‡ gdt@asterix.cernet.cr

1. Introduction

The Schrödinger equation plays a central role in atomic physics, providing a simple, but effective, first approximation description of the spectrum and wavefunctions of bound states in quantum electrodynamics. It can be systematically improved in QED, leading to an exact quantum field theoretic description of atomic states such as positronium and muonium as given by the relativistic Bethe–Salpeter equation.

A long-sought goal in hadron physics is to find a simple analytic first approximation to QCD analogous to the Schrödinger–Coulomb equation of atomic physics. This problem is particularly challenging since the formalism must be relativistic, color-confining, and consistent with chiral symmetry.

We have recently shown that the soft-wall AdS/QCD model, modified by a positive-sign dilaton metric, leads to a remarkable one-parameter description of nonperturbative hadron dynamics. The model predicts a zero-mass pion for zero-mass quarks and a Regge spectrum of linear trajectories with the same slope in the leading orbital angular momentum L of hadrons and the radial quantum number N .

Light-front holography [1] maps the amplitudes which are functions of the fifth dimension variable z of Anti-de Sitter (AdS) space to a corresponding hadron theory quantized at fixed light-front time $\tau = x^0 + x^3/c$, the time marked by the front of a light wave [2]. The resulting Lorentz-invariant relativistic light-front (LF) wave equations are functions of an impact variable ζ which measures the invariant separation of the quark and gluonic constituents within the hadron at equal light-front time; it is analogous to the radial coordinate r in the Schrödinger equation. This novel approach leads to a semiclassical frame-independent first approximation to the spectrum and light-front wavefunctions of meson and baryon light-quark bound states, which in turn predict the behavior of the pion and nucleon form factors in the space-like and time-like regions. The resulting equation for a meson $q\bar{q}$ bound state has the form of a relativistic Lorentz invariant Schrödinger equation

$$\left(-\frac{d^2}{d\zeta^2} - \frac{1 - 4L^2}{4\zeta^2} + U(\zeta) \right) \phi(\zeta) = \mathcal{M}^2 \phi(\zeta), \quad (1)$$

where the confining potential is $U(\zeta) = \kappa^4 \zeta^2 + 2\kappa^2(L + S - 1)$ in a soft dilaton modified background [3]. There is only one parameter, the mass scale $\kappa \sim 1/2$ GeV, which enters the confinement potential. Here $S = 0, 1$ is the spin of the q and \bar{q} . In a relativistic theory, the hadron eigenstate has components of different orbital angular momentum, just as in the Dirac–Coulomb equation, where the lowest eigenstate has both S and P states. By convention one uses the minimum L to label the state. Furthermore, in light-front theory, the label L refers to the maximum orbital angular projection $|L^z|$, of the bound state.

The single-variable LF Schrödinger equation, Eq. (1), determines the eigenspectrum and the light-front wavefunctions (LFWFs) of hadrons for general spin and orbital angular momentum [1]. This LF wave equation serves as a semiclassical first approximation to QCD, and it is equivalent to the equations of motion which describe the propagation of spin- J modes in AdS space. Light-front holography thus provides a remarkable connection between the description of hadronic modes in AdS space and the Hamiltonian formulation of QCD in physical space-time quantized on the light-front at fixed LF time τ . If one further chooses the constituent rest frame (CRF) [4–6], where the total 3-momentum vanishes: $\sum_{i=1}^n \mathbf{k}_i = 0$, then the kinetic energy in the LF wave equation displays the usual 3-dimensional rotational invariance.

The meson spectrum predicted by Eq. (1) has a string-theory Regge form $M^2 = 4\kappa^2(n + L + S/2)$; *i.e.*, the square of the eigenmasses are linear in both L and n , where n counts the number of nodes of the wavefunction in the radial variable ζ . This is illustrated for the pseudoscalar and vector-meson spectra in Figs. 1 and 2, where the data are from Ref. [7]. The pion ($S = 0, n = 0, L = 0$) is massless for zero quark mass, consistent with chiral invariance. Thus one can compute the hadron spectrum by simply adding $4\kappa^2$ for a unit change in the radial quantum number, $4\kappa^2$ for a change in one unit in the orbital quantum number and $2\kappa^2$ for a change of one unit of spin S . Remarkably, the same rule holds for baryons as we shall show below. For other recent calculations of the hadronic spectrum based on AdS/QCD, see Refs. [8–25].

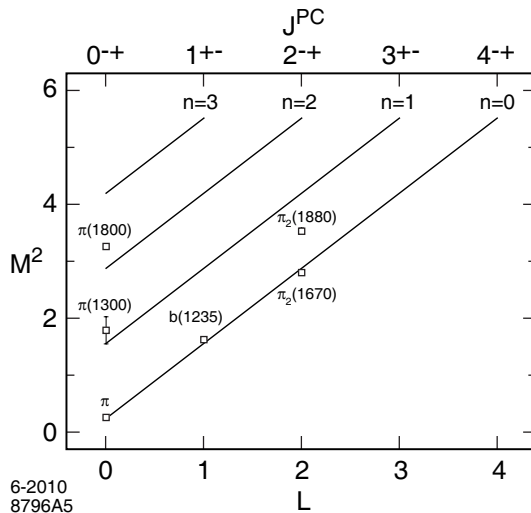


Fig. 1. Parent and daughter Regge trajectories for the π -meson family for $\kappa = 0.6$ GeV.

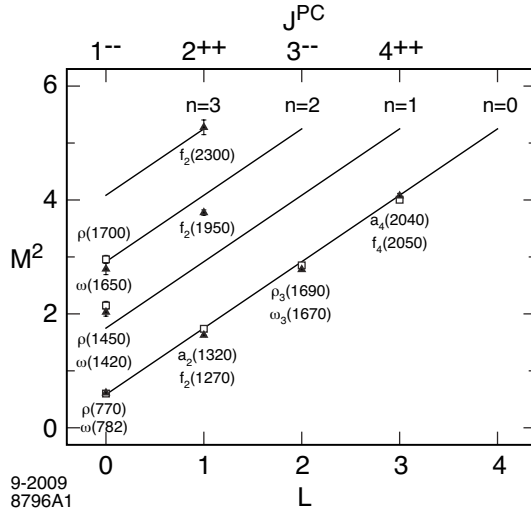


Fig. 2. Regge trajectories for the $I = 1$ ρ -meson and the $I = 0$ ω -meson families for $\kappa = 0.54$ GeV.

The eigensolutions of Eq. (1) provide the light-front wavefunctions of the valence Fock state of the hadrons $\psi(\zeta) = \psi(x, \mathbf{b}_\perp)$ as illustrated for the pion in Fig. 3 for the soft and hard wall models. Given these wavefunctions, one can predict many hadronic observables such as the generalized parton distributions that control deeply virtual Compton scattering. For example, hadron form factors can be predicted from the overlap of LFWFs as in the Drell–Yan–West formula. The prediction for the space-like pion form factor is shown in Fig. 4. The vector–meson poles residing in the dressed current in the soft-wall model require choosing a value of κ smaller by a factor $\frac{1}{\sqrt{2}}$ than the canonical value of κ that determines the mass scale of the hadronic spectra. This shift is apparently related to the fact that the longitudinal twist-3 current J^+ , which appears in the Drell–Yan expression for the space-like form factor, is different from the leading-twist $q\bar{q}$ operator that is used to compute the vector–meson spectrum. The leading-twist operator corresponds to the transverse current J_\perp which is responsible for producing the $\bar{q}q$ state in the time-region from e^+e^- annihilation. We will discuss this point further in an upcoming paper. Other recent computations of the space-like pion form factor in AdS/QCD are presented in [29,30]. Given the LFWFs one can compute jet hadronization at the amplitude level from first principles [31]. A similar method has been used to predict the production of antihydrogen from the off-shell coalescence of relativistic antiprotons and positrons [32].

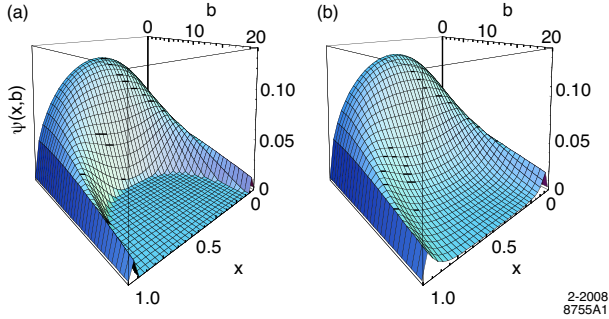


Fig. 3. Pion light-front wavefunction $\psi_\pi(x, \mathbf{b}_\perp)$ for the AdS/QCD (a) hard-wall ($\Lambda_{\text{QCD}} = 0.32 \text{ GeV}$) and (b) soft-wall ($\kappa = 0.375 \text{ GeV}$) models.

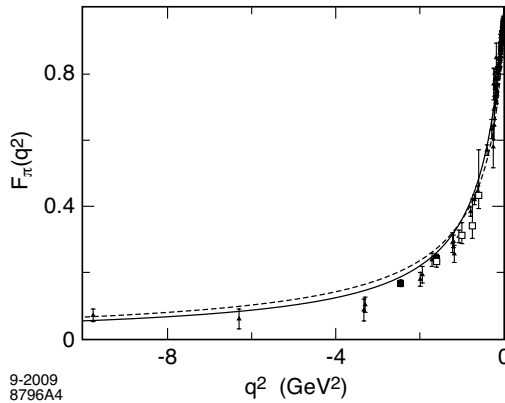


Fig. 4. Space-like scaling behavior for $F_\pi(Q^2)$ as a function of q^2 . The continuous line is the prediction of the soft-wall model for $\kappa = 0.375 \text{ GeV}$. The dashed line is the prediction of the hard-wall model for $\Lambda_{\text{QCD}} = 0.22 \text{ GeV}$. The triangles are the data compilation from Baldini *et al.* [26] the filled boxes are JLAB 1 data [27] and empty boxes are JLAB 2 data [28].

This semi-classical first approximation to QCD can be systematically improved by using the complete orthonormal solutions of Eq. (1) to diagonalize the QCD light-front Hamiltonian [33] or by applying the Lippmann–Schwinger method to systematically include the QCD interaction terms. In either case, the result is the full Fock state structure of the hadron eigen-solution. One can also model heavy-light and heavy hadrons by including non-zero quark masses in the LF kinetic energy $\sum_i (\mathbf{k}_{\perp i}^2 + m_i^2)/x_i$ as well as the effects of the one-gluon exchange potential.

One can derive these results in two parallel ways. In the first method, one begins with a conformal approximation to QCD, justified by evidence that the theory has an infrared fixed point [34]. One then uses the fact that

the conformal group has a geometrical representation in the five-dimensional AdS₅ space to model an effective dual gravity description in AdS. The fact that conformal invariance is reflected in the isometries of AdS is an essential ingredient of Maldacena's AdS/CFT correspondence [35]. Confinement is effectively introduced with a sharp cut-off in the infrared region of AdS space, the "hard-wall" model [36] or with a dilaton background in the fifth dimension which produces a smooth cutoff and linear Regge trajectories, the "soft-wall" model [37]. The soft-wall AdS/CFT model with a dilaton-modified AdS space leads to the potential $U(z) = \kappa^4 z^2 + 2\kappa^2(L + S - 1)$. This potential can be derived directly from the action in AdS space [3] and corresponds to a dilaton profile $\exp(+\kappa^2 z^2)$, with a positive argument of the exponential, opposite in sign to that of Ref. [37]. The modified metric induced by the dilaton can be interpreted in AdS space as a gravitational potential for an object of mass m in the fifth dimension: $V(z) = mc^2 \sqrt{g_{00}} = mc^2 R e^{\pm \kappa^2 z^2/2} / z$. In the case of the negative solution, the potential decreases monotonically, and thus an object in AdS will fall to infinitely large values of z . For the positive solution, the potential is non-monotonic and has an absolute minimum at $z_0 = 1/\kappa$. Furthermore, for large values of z the gravitational potential increases exponentially, confining any object to distances $\langle z \rangle \sim 1/\kappa$ [3]. We will thus choose the confining positive sign dilaton solution [3, 38] with opposite sign to that of Ref. [37]. This additional warp factor leads to a well-defined scale-dependent effective coupling.

Glazek and Schaden [39] have shown that a harmonic-oscillator confining potential naturally arises as an effective potential between heavy quark states when one stochastically eliminates higher gluonic Fock states. Also, Hoyer [40] has argued that the Coulomb and linear potentials are uniquely allowed in the Dirac equation at the lowest level in \hbar . The linear potential becomes a harmonic oscillator potential in the corresponding Klein–Gordon equation.

Hadrons are identified in AdS/QCD by matching the power behavior of the hadronic amplitude at the AdS boundary at small z to the twist of its interpolating operator at short distances $x^2 \rightarrow 0$, as required by the AdS/CFT dictionary. The twist corresponds to the dimension of fields appearing in chiral super-multiplets [41]. The canonical twist of a hadron equals the number of its constituents. We can then apply light-front holography to relate the amplitude eigensolutions in the fifth dimension coordinate z to the LF wavefunctions in the physical space-time variable ζ . Light-front holography can be derived by establishing an identity between the Polchinski–Strassler formula for current matrix elements in AdS space [42] and the corresponding Drell–Yan–West formula in LF theory [43, 44]. The same correspondence is obtained for both electromagnetic [45, 46] and gravitational form factors, [47] a nontrivial test of consistency.

In the second method we use a first semiclassical approximation to transform the fixed LF time bound-state Hamiltonian equation to a corresponding wave equation in AdS space. The invariant LF coordinate ζ allows the separation of the dynamics of quark and gluon binding from the kinematics of constituent spin and internal orbital angular momentum [1]. In effect, ζ represents the off-light-front energy shell (invariant mass) dependence of the bound state. The result is the single-variable LF relativistic Schrödinger equation which determines the spectrum and LFWFs of hadrons for general spin and orbital angular momentum. This LF wave equation serves as a semiclassical first approximation to QCD, and it is equivalent to the equations of motion which describe the propagation of spin- J modes in AdS space.

The term $L^2/4\zeta^2$ in the LF equation of motion (1) is derived from the reduction of the LF kinetic energy, when one transforms to the radial ζ and angular coordinate φ , in analogy to the $\ell(\ell + 1)/r^2$ Casimir term in Schrödinger theory. One thus establishes the interpretation of the orbital angular momentum L in the AdS equations of motion. The interaction terms build confinement and correspond to truncation of AdS space in an effective dual gravity approximation [1]. The duality between these two methods provides a direct connection between the description of hadronic modes in AdS space and the Hamiltonian formulation of QCD in physical space-time, quantized on the light-front at fixed LF time τ .

2. Foundations of AdS/QCD

One of the most significant theoretical advances in recent years has been the application of the AdS/CFT correspondence [35] between string theories defined in 5-dimensional Anti-de Sitter space-time and conformal field theories in physical space-time, to study the dynamics of strongly coupled quantum field theories. The essential principle underlying the AdS/CFT approach to conformal gauge theories is the isomorphism of the group of Poincaré and conformal transformations $SO(4, 2)$ to the group of isometries of Anti-de Sitter space. The AdS metric is

$$ds^2 = \frac{R^2}{z^2} (\eta_{\mu\nu} dx^\mu dx^\nu - dz^2) , \quad (2)$$

which is invariant under scale changes of the coordinate in the fifth dimension $z \rightarrow \lambda z$ and $x_\mu \rightarrow \lambda x_\mu$. Thus one can match scale transformations of the theory in $3 + 1$ physical space-time to scale transformations in the fifth dimension z . In the AdS/CFT duality, the amplitude $\Phi(z)$ represents the extension of the hadron into the additional fifth dimension. The behavior of $\Phi(z) \rightarrow z^\tau$ at $z \rightarrow 0$ matches the twist-dimension τ of the hadron at short distances.

In the standard applications of AdS/CFT methods, one begins with Maldacena's duality between the conformal supersymmetric $SO(4, 2)$ gauge theory and a semiclassical supergravity string theory defined in a 10 dimension $AdS_5 \times S^5$ space-time. There are no existing string theories actually dual to QCD, but nevertheless many interesting predictions can be made. In contrast, in our approach, we simply use the mathematical fact that the effects of scale transformations in a conformal theory can be mapped to the z -dependence of amplitudes in AdS_5 space. In this approach, we consider the propagation of hadronic modes in a fixed effective gravitational background which encodes salient properties of the QCD dual theory, such as the ultraviolet conformal limit at the AdS boundary at $z \rightarrow 0$, as well as modifications of the background geometry in the large- z infrared region, characteristic of strings dual to confining gauge theories.

The identification of orbital angular momentum of the constituents is a key element in the description of the internal structure of hadrons using holographic principles. In our approach quark and gluon degrees of freedom are explicitly introduced in the gauge/gravity correspondence, in contrast with the usual AdS/QCD framework [48, 49] where axial and vector currents become the primary entities as in effective chiral theory. In our approach, the holographic mapping is carried out in the strongly coupled regime where QCD is almost conformal corresponding to an infrared fixed-point. Our analysis follows from developments in light-front QCD [1, 45–47, 50, 51] which have been inspired by the AdS/CFT correspondence [35].

QCD is not conformal, but there is in fact much empirical evidence from lattice gauge theory [52], Dyson Schwinger theory [53], and empirical effective charges [54] that the QCD β -function vanishes in the infrared [34]. The QCD infrared fixed point arises since the propagators of the confined quarks and gluons in the loop integrals contributing to the β -function have a maximal wavelength [55]. The decoupling of quantum loops in the infrared is analogous to QED where vacuum polarization corrections to the photon propagator decouple at $Q^2 \rightarrow 0$. Since there is a window where the QCD coupling is large and approximately constant, QCD resembles a conformal theory for massless quarks. Thus, even though QCD is not conformally invariant, one can use the mathematical representation of the conformal group in five-dimensional Anti-de Sitter space to construct an analytic first approximation to the theory. One then uses AdS_5 to represent scale transformations within the conformal window. Unlike the top-down supergravity approach, one is not limited to hadrons of spin $J \leq 2$ in our bottom-up approach, and one can study baryons with $N_C = 3$. The theory also predicts dimensional counting for form factors and other fixed CM angle exclusive reactions. Moreover, as we shall review, light-front holography allows one to map the hadronic amplitudes $\Phi(z)$ determined in the AdS fifth dimension z to the valence LFWFs of each hadron as a function of a covariant

impact variable ζ . Moreover, the same techniques provide a prediction for the QCD coupling $\alpha_s(Q^2)$ and its β -function which reflects the dynamics of confinement.

3. Light-front quantization

Light-front quantization is the ideal framework for describing the structure of hadrons in terms of their quark and gluon degrees of freedom. The light-front wavefunctions of bound states in QCD are relativistic generalizations of the Schrödinger wavefunctions, but they are determined at fixed light-front time $\tau = x^+ = x^0 + x^3$, the time marked by the front of a light wave [2], rather than at fixed ordinary time t . They play the same role in hadron physics that Schrödinger wavefunctions play in atomic physics. In addition, the simple structure of the LF vacuum provides an unambiguous definition of the partonic content of a hadron in QCD.

We can define the LF Lorentz invariant Hamiltonian $H_{\text{LF}} = P_\mu P^\mu = P^- P^+ - \mathbf{P}_\perp^2$ with eigenstates $|\psi_{\text{H}}(P^+, \mathbf{P}_\perp, S_z)\rangle$ and eigenmass \mathcal{M}_{H}^2 , the mass spectrum of the color-singlet states of QCD [56]. H_{LF} can be determined canonically from the QCD Lagrangian in light-cone gauge $A^+ = 0$. The light-front formalism for gauge theories in light-cone gauge is particularly useful in that there are no ghosts and one has a direct physical interpretation of orbital angular momentum. The Heisenberg equation for QCD on the light-front thus takes the form $H_{\text{LF}}|\psi_{\text{H}}\rangle = \mathcal{M}_{\text{H}}^2|\psi_{\text{H}}\rangle$. Its eigenfunctions are the light-front eigenstates which define the frame-independent light-front wavefunctions, and its eigenvalues yield the hadronic spectrum, the bound states as well as the continuum. A state $|\psi_{\text{H}}\rangle$ is an expansion in multiparticle Fock states $|n\rangle$ of the free LF Hamiltonian: $|\psi_{\text{H}}\rangle = \sum_n \psi_{n/\text{H}}|n\rangle$, where a one parton state is $|q\rangle = \sqrt{2q^+} b^\dagger(q)|0\rangle$. The projection of the eigensolutions on the free Fock basis thus give the n -parton LF wavefunctions $\psi_{n/\text{H}} = \langle n|\psi_{\text{H}}\rangle$ needed for phenomenology.

Light-front quantization of QCD provides a nonperturbative method for solving QCD in Minkowski space. Unlike lattice gauge theories, fermions introduce no new complications. Heisenberg's problem on the light-front can be solved numerically using discretized light-front quantization (DLCQ) [57] by applying anti-periodic boundary conditions in $\sigma = x^0 - x^3$. This method has been used successfully to solve many lower dimension quantum field theories [56].

4. Light-front wavefunctions

The Schrödinger wavefunction describes the quantum-mechanical structure of an atomic system at the amplitude level. The light-front multiparticle Fock state wavefunctions play a similar role in quantum chromodynamics,

providing a fundamental description of the structure and internal dynamics of hadrons in terms of their constituent quarks and gluons. The LFWFs of bound states in QCD are relativistic generalizations of the Schrödinger wavefunctions of atomic physics, but they are determined at fixed light-cone time $\tau = x^0 + x^3/c$ — the “front form” introduced by Dirac [2] — rather than at fixed ordinary time t .

When a flash from a camera illuminates a scene, each object is illuminated along the light-front of the flash; *i.e.*, at a given τ . Similarly, when a sample is illuminated by an X-ray source, each element of the target is struck at a given τ . In contrast, setting the initial condition using conventional instant time t requires simultaneous scattering of photons on each constituent. Thus it is natural to set boundary conditions at fixed τ and then evolve the system using the light-front Hamiltonian $P^- = P^0 - P^3 = id/d\tau$. The invariant Hamiltonian $H_{\text{LF}} = P^+P^- - \mathbf{P}_\perp^2$ then has eigenvalues \mathcal{M}^2 , where \mathcal{M} is the physical mass. Its eigenfunctions are the light-front eigenstates whose Fock state projections define the light-front wavefunctions. Given the LF Fock state wavefunctions $\psi_n^{\text{H}}(x_i, \mathbf{k}_\perp i, \lambda_i)$, where $x_i = k^+/P^+$, $\sum_{i=1}^n x_i = 1$, $\sum_{i=1}^n \mathbf{k}_\perp i = 0$, one can immediately compute observables such as hadronic form factors (overlaps of LFWFs), structure functions (squares of LFWFS), as well as the generalized parton distributions and distribution amplitudes which underly hard exclusive reactions.

The most useful feature of LFWFs is the fact that they are frame-independent; *i.e.*, the form of the LFWF is independent of the hadron’s total momentum $P^+ = P^0 + P^z$ and \mathbf{P}_\perp . The simplicity of Lorentz boosts of LFWFs contrasts dramatically with the complexity of the boost of wavefunctions defined at fixed time t [58]. Light-front quantization is thus the ideal framework to describe the structure of hadrons in terms of their quark and gluon degrees of freedom. The constituent spin and orbital angular momentum properties of the hadrons are also encoded in the LFWFs. The total angular momentum projection [59], $J^z = \sum_{i=1}^n S_i^z + \sum_{i=1}^{n-1} L_i^z$, is conserved Fock-state by Fock-state and by every interaction in the LF Hamiltonian.

The angular momentum projections in the LF \hat{z} direction L^z, S^z and J^z are kinematical in the front form, so they are the natural quantum numbers to label the eigenstates of light-front physics. In the massless fermion limit, the gauge interactions conserve LF chirality; *i.e.*, the quark spin S^z is conserved (rather than helicity $\vec{S} \cdot \vec{p}$) at the QCD vertices. Similarly, quark–antiquark pairs from gluon splitting have opposite S^z . For example, the light-front wavefunction of a massless electron at order α in QED with $J^z = +1/2$ has fermion–photon Fock components $S_e^z = +1/2, S_\gamma^z = +1, L^z = -1$ and $S_e^z = +1/2, S_\gamma^z = -1, L^z = +1$.

In general, a hadronic eigenstate with spin j in the front form corresponds to an eigenstate of $J^2 = j(j+1)$ in the rest frame in the conventional instant form. It thus has $2j+1$ degenerate states with $J^z =$

$-j, -j + 1, \dots, j - 1, +j$ [56]. An important feature of relativistic theories is that hadron eigenstates have in general Fock components with different L components. For example, the $S^z = +1/2$ proton eigenstate in AdS space has equal probability $S_q^z = +1/2, L^z = 0$ and $S_q^z = -1/2, L^z = +1$ light-front Fock components with equal probability. Thus in AdS, the proton is effectively a quark/scalar–diquark composite with equal S and P waves.

In the case of QED, the ground $1S$ state of the Dirac–Coulomb equation has both $L = 0$ and $L = 1$ components. By convention, in both light-front QCD and QED, one labels the eigenstate with its minimum value of L . For example, the symbol L in the AdS/QCD spectral prediction $M^2 = 4\kappa^2(n + L + S/2)$ refers to the *minimum* L , and $S = j$ is the total spin of the hadron.

Other advantageous features of light-front quantization include:

- The simple structure of the light-front vacuum allows an unambiguous definition of the partonic content of a hadron in QCD. The chiral and gluonic condensates are properties of the higher Fock states [60, 61] rather than the vacuum. In the case of the Higgs model, the effect of the usual Higgs vacuum expectation value is replaced by a constant $k^+ = 0$ zero mode field [62]. The LF vacuum is trivial up to zero modes in the front form, thus eliminating contributions to the cosmological constant from QED or QCD [61]. We discuss the remarkable consequences of this for the cosmological constant in Section 14.
- If one quantizes QCD in the physical light-cone gauge (LCG) $A^+ = 0$, then gluons only have physical angular momentum projections $S^z = \pm 1$. The orbital angular momenta of quarks and gluons are defined unambiguously, and there are no ghosts.
- The gauge-invariant distribution amplitude $\phi(x, Q)$ is the integral of the valence LFWF in LCG integrated over the internal transverse momentum $k_\perp^2 < Q^2$ because the Wilson line is trivial in this gauge. It is also possible to quantize QCD in Feynman gauge in the light front [63].
- LF Hamiltonian perturbation theory provides a simple method for deriving analytic forms for the analog of Parke–Taylor amplitudes [64], where each particle spin S^z is quantized in the LF z direction. The gluonic g^6 amplitude $T(-1 - 1 \rightarrow +1 + 1 + 1 + 1 + 1 + 1)$ requires $\Delta L^z = 8$; it thus must vanish at tree level since each three-gluon vertex has $\Delta L^z = \pm 1$. However, the order g^8 one-loop amplitude can be non-zero.
- Amplitudes in light-front perturbation theory may be automatically renormalized using the “alternate denominator” subtraction method [65]. The application to QED has been checked at one and two loops [65].

- A fundamental theorem for gravity can be derived from the equivalence principle: the anomalous gravitomagnetic moment defined from the spin-flip matrix element of the energy-momentum tensor is identically zero, $B(0) = 0$ [66]. This theorem can be proven in the light-front formalism Fock state by Fock state [59].
- LFWFs obey the cluster decomposition theorem, providing an elegant proof of this theorem for relativistic bound states [67].
- The LF Hamiltonian can be diagonalized using the discretized light-cone quantization (DLCQ) method [57]. This nonperturbative method is particularly useful for solving low-dimension quantum field theories such as QCD(1 + 1) [68].
- LF quantization provides a distinction between static (the square of LFWFs) distributions *versus* non-universal dynamic structure functions, such as the Sivers single-spin correlation and diffractive deep inelastic scattering which involve final state interactions. The origin of nuclear shadowing and process independent anti-shadowing also becomes explicit.
- LF quantization provides a simple method to implement jet hadronization at the amplitude level.
- The instantaneous fermion interaction in LF quantization provides a simple derivation of the $J = 0$ fixed pole contribution to deeply virtual Compton scattering [69] *i.e.*, the $e_q^2 s^0 F(t)$ contribution to the DVCS amplitude which is independent of photon energy and virtuality.
- Unlike instant time quantization, the bound state Hamiltonian equation of motion in the LF is frame independent. This makes a direct connection of QCD with AdS/CFT methods possible [1].

5. Applications of light-front wavefunctions

The Fock components $\psi_{n/H}(x_i, \mathbf{k}_{\perp i}, \lambda_i^z)$ are independent of P^+ and \mathbf{P}_{\perp} and depend only on relative partonic coordinates: the momentum fraction $x_i = k_i^+/P^+$, the transverse momentum $\mathbf{k}_{\perp i}$ and spin component λ_i^z . The LFWFs $\psi_{n/H}$ provide a *frame-independent* representation of a hadron which relates its quark and gluon degrees of freedom to their asymptotic hadronic state. Since the LFWFs are independent of the hadron's total momentum $P^+ = P^0 + P^3$, so that once they are known in one frame, they are known in all frames; Wigner transformations and Melosh rotations are not required. They also allow one to formulate hadronization in inclusive and exclusive reactions at the amplitude level.

A key example of the utility of the light-front formalism is the Drell–Yan–West formula [43, 44] for the space-like form factors of electromagnetic currents given as overlaps of initial and final LFWFs. At high momentum, where one can iterate the hard scattering kernel, this yields the dimensional counting rules, factorization theorems, and ERBL evolution of the distribution amplitudes. The gauge-invariant distribution amplitudes $\phi_H(x_i, Q)$ defined from the integral over the transverse momenta $\mathbf{k}_{\perp i}^2 \leq Q^2$ of the valence (smallest n) Fock state provide a fundamental measure of the hadron at the amplitude level [70, 71]; they are the nonperturbative inputs to the factorized form of hard exclusive amplitudes and exclusive heavy hadron decays in pQCD.

Given the light-front wavefunctions $\psi_{n/H}$ one can compute a large range of other hadron observables. For example, the valence and sea quark and gluon distributions which are measured in deep inelastic lepton scattering are defined from the squares of the LFWFs summed over all Fock states n . Exclusive weak transition amplitudes [72] such as $B \rightarrow \ell\nu\pi$, and the generalized parton distributions [73] measured in deeply virtual Compton scattering $\gamma^*p \rightarrow \gamma p$ are (assuming the “handbag” approximation) overlaps of the initial and final LFWFs with $n = n'$ and $n = n' + 2$. The resulting distributions obey the DGLAP and ERBL evolution equations as a function of the maximal invariant mass, thus providing a physical factorization scheme [74]. In each case, the derived quantities satisfy the appropriate operator product expansions, sum rules, and evolution equations. At large x , where the struck quark is far-off shell, DGLAP evolution is quenched [75] so that the fall-off of the DIS cross-sections in Q^2 satisfies Bloom–Gilman inclusive–exclusive duality at fixed W^2 .

The simple features of the light-front contrast with the conventional instant form where one quantizes at $t = 0$. For example, calculating a hadronic form factor requires boosting the hadron’s wavefunction from the initial to final state, a dynamical problem as difficult as solving QCD itself. Moreover, current matrix elements require computing the interaction of the probe with all of connected currents fluctuating in the QCD vacuum. Each contributing diagram is frame-dependent.

6. Light-front holography

Light-front holography [1, 45–47, 76] maps a confining gauge theory quantized on the light front to a higher-dimensional Anti-de Sitter space incorporating the AdS/CFT correspondence as a useful guide. This correspondence provides a direct connection between the hadronic amplitudes $\Phi(z)$ in AdS space with LF wavefunctions $\phi(\zeta)$ describing the quark and gluon constituent structure of hadrons in physical space-time. In the case of a meson, $\zeta = \sqrt{x(1-x)\mathbf{b}_{\perp}^2}$ is a Lorentz invariant coordinate which measures

the distance between the quark and antiquark; it is analogous to the radial coordinate r in the Schrödinger equation. Here \mathbf{b}_\perp is the Fourier conjugate of the transverse momentum \mathbf{k}_\perp . The variable ζ also represents the off-light-front energy shell and invariant mass dependence of the bound state. Light-front holography provides a connection between the description of hadronic modes in AdS space and the Hamiltonian formulation of QCD in physical space-time quantized on the light-front at fixed LF time τ . The resulting equation for the mesonic $q\bar{q}$ bound states at fixed light-front time, Eq. (1), has the form of a single-variable relativistic Lorentz invariant Schrödinger equation [1]. The resulting light-front eigenfunctions provide a fundamental description of the structure and internal dynamics of hadronic states in terms of their constituent quark and gluons.

7. Holographic mapping of transition amplitudes

The mapping between the LF invariant variable ζ and the fifth-dimension AdS coordinate z was originally obtained by matching the expression for electromagnetic current matrix elements in AdS space with the corresponding expression for the current matrix element, using LF theory in physical space-time [45]. It has also been shown that one obtains the identical holographic mapping using the matrix elements of the energy-momentum tensor [47, 77] thus verifying the consistency of the holographic mapping from AdS to physical observables defined on the light front.

The light-front electromagnetic form factor in impact space [45, 46, 78] can be written as a sum of overlap of light-front wave functions of the $j = 1, 2, \dots, n - 1$ spectator constituents

$$F(q^2) = \sum_n \prod_{j=1}^{n-1} \int dx_j d^2\mathbf{b}_{\perp j} \sum_q e_q \exp\left(i\mathbf{q}_\perp \cdot \sum_{j=1}^{n-1} x_j \mathbf{b}_{\perp j}\right) |\psi_{n/H}(x_j, \mathbf{b}_{\perp j})|^2, \quad (3)$$

where the normalization is defined by

$$\sum_n \prod_{j=1}^{n-1} \int dx_j d^2\mathbf{b}_{\perp j} |\psi_{n/H}(x_j, \mathbf{b}_{\perp j})|^2 = 1. \quad (4)$$

The formula is exact if the sum is over all Fock states n . For definiteness we shall consider a two-quark π^+ valence Fock state $|u\bar{d}\rangle$ with charges $e_u = 2/3$ and $e_{\bar{d}} = 1/3$. For $n = 2$, there are two terms which contribute to the q -sum in (3). Exchanging $x \leftrightarrow 1 - x$ in the second integral we find

$$F_{\pi^+}(q^2) = 2\pi \int_0^1 \frac{dx}{x(1-x)} \int \zeta d\zeta J_0\left(\zeta q \sqrt{\frac{1-x}{x}}\right) \left| \psi_{u\bar{d}/\pi}(x, \zeta) \right|^2, \quad (5)$$

where $\zeta^2 = x(1-x)\mathbf{b}_\perp^2$ and $F_{\pi^+}(q=0) = 1$.

We now compare this result with the electromagnetic form-factor in AdS space [42]

$$F(Q^2) = R^3 \int \frac{dz}{z^3} J(Q^2, z) |\Phi(z)|^2, \tag{6}$$

where $J(Q^2, z) = zQK_1(zQ)$. Using the integral representation of $J(Q^2, z)$

$$J(Q^2, z) = \int_0^1 dx J_0 \left(\zeta Q \sqrt{\frac{1-x}{x}} \right) \tag{7}$$

we write the AdS electromagnetic form-factor as

$$F(Q^2) = R^3 \int_0^1 dx \int \frac{dz}{z^3} J_0 \left(zQ \sqrt{\frac{1-x}{x}} \right) |\Phi(z)|^2. \tag{8}$$

Comparing with the light-front QCD form factor (5) for arbitrary values of Q [45]

$$|\psi(x, \zeta)|^2 = \frac{R^3}{2\pi} x(1-x) \frac{|\Phi(\zeta)|^2}{\zeta^4}, \tag{9}$$

where we identify the transverse LF variable ζ , $0 \leq \zeta \leq \Lambda_{\text{QCD}}$, with the holographic variable z . Identical results are obtained from the mapping of the QCD gravitational form factor with the expression for the hadronic gravitational form factor in AdS space [47, 77].

8. A semiclassical approximation to QCD

One can also derive light-front holography using a first semiclassical approximation to transform the fixed light-front time bound-state Hamiltonian equation of motion in QCD to a corresponding wave equation in AdS space [1]. To this end we compute the invariant hadronic mass \mathcal{M}^2 from the hadronic matrix element

$$\langle \psi_{\text{H}}(P') | H_{\text{LF}} | \psi_{\text{H}}(P) \rangle = \mathcal{M}_{\text{H}}^2 \langle \psi_{\text{H}}(P') | \psi_{\text{H}}(P) \rangle \tag{10}$$

expanding the initial and final hadronic states in terms of its Fock components. We use the frame $P = (P^+, M^2/P^+, \vec{0}_{\perp})$, where $H_{\text{LF}} = P^+ P^-$. The LF expression for \mathcal{M}^2 In impact space is

$$\begin{aligned} \mathcal{M}_{\text{H}}^2 = & \sum_n \prod_{j=1}^{n-1} \int dx_j d^2\mathbf{b}_{\perp j} \psi_n^*(x_j, \mathbf{b}_{\perp j}) \sum_q \left(\frac{-\nabla_{\mathbf{b}_{\perp q}}^2 + m_q^2}{x_q} \right) \psi_n(x_j, \mathbf{b}_{\perp j}) \\ & +(\text{interactions}) \end{aligned} \tag{11}$$

plus similar terms for antiquarks and gluons ($m_g = 0$).

To simplify the discussion we will consider a two-parton hadronic bound state. In the limit of zero quark mass $m_q \rightarrow 0$

$$\mathcal{M}^2 = \int_0^1 \frac{dx}{x(1-x)} \int d^2\mathbf{b}_\perp \psi^*(x, \mathbf{b}_\perp) (-\nabla_{\mathbf{b}_\perp}^2) \psi(x, \mathbf{b}_\perp) + (\text{interactions}). \quad (12)$$

The functional dependence for a given Fock state is given in terms of the invariant mass

$$\mathcal{M}_n^2 = \left(\sum_{a=1}^n k_a^\mu \right)^2 = \sum_a \frac{\mathbf{k}_{\perp a}^2 + m_a^2}{x_a} \rightarrow \frac{\mathbf{k}_\perp^2}{x(1-x)} \quad (13)$$

the measure of the off-mass shell energy $\mathcal{M}^2 - \mathcal{M}_n^2$ of the bound state. Similarly in impact space the relevant variable for a two-parton state is $\zeta^2 = x(1-x)\mathbf{b}_\perp^2$. Thus, to first approximation LF dynamics depend only on the boost invariant variable \mathcal{M}_n or ζ , and hadronic properties are encoded in the hadronic mode $\phi(\zeta)$ from the relation

$$\psi(x, \zeta, \varphi) = e^{iM\varphi} X(x) \frac{\phi(\zeta)}{\sqrt{2\pi\zeta}}, \quad (14)$$

thus factoring out the angular dependence φ and the longitudinal, $X(x)$, and transverse mode $\phi(\zeta)$ with normalization $\langle \phi | \phi \rangle = \int d\zeta |\langle \zeta | \phi \rangle|^2 = 1$.

We can write the Laplacian operator in (12) in circular cylindrical coordinates (ζ, φ) and factor out the angular dependence of the modes in terms of the SO(2) Casimir representation L^2 , $L = L^z$, of orbital angular momentum in the transverse plane. Using (14) we find [1]

$$\mathcal{M}^2 = \int d\zeta \phi^*(\zeta) \sqrt{\zeta} \left(-\frac{d^2}{d\zeta^2} - \frac{1}{\zeta} \frac{d}{d\zeta} + \frac{L^2}{\zeta^2} \right) \frac{\phi(\zeta)}{\sqrt{\zeta}} + \int d\zeta \phi^*(\zeta) U(\zeta) \phi(\zeta), \quad (15)$$

where all the complexity of the interaction terms in the QCD Lagrangian is summed up in the effective potential $U(\zeta)$. The LF eigenvalue equation $H_{\text{LF}}|\phi\rangle = \mathcal{M}^2|\phi\rangle$ is thus a light-front wave equation for ϕ

$$\left(-\frac{d^2}{d\zeta^2} - \frac{1-4L^2}{4\zeta^2} + U(\zeta) \right) \phi(\zeta) = \mathcal{M}^2 \phi(\zeta), \quad (16)$$

an effective single-variable light-front Schrödinger equation which is relativistic, covariant and analytically tractable. It is important to notice that in the light-front the SO(2) Casimir for orbital angular momentum L^2 is a kinematical quantity, in contrast with the usual SO(3) Casimir $\ell(\ell+1)$ from non-relativistic physics which is rotational, but not boost invariant.

Using (11) one can readily generalize the equations to allow for the kinetic energy of massive quarks [79]. In this case, however, the longitudinal mode $X(x)$ does not decouple from the effective LF bound-state equations.

As the simplest example, we consider a bag-like model where partons are free inside the hadron and the interaction terms effectively build confinement. The effective potential is a hard wall: $U(\zeta) = 0$ if $\zeta \leq 1/\Lambda_{\text{QCD}}$ and $U(\zeta) = \infty$ if $\zeta > 1/\Lambda_{\text{QCD}}$, where boundary conditions are imposed on the boost invariant variable ζ at fixed light-front time. If $L^2 \geq 0$ the LF Hamiltonian is positive definite $\langle \phi | H_{\text{LF}} | \phi \rangle \geq 0$ and thus $\mathcal{M}^2 \geq 0$. If $L^2 < 0$ the bound state equation is unbounded from below and the particle “falls towards the center”. The critical value corresponds to $L = 0$. The mode spectrum follows from the boundary conditions $\phi(\zeta = 1/\Lambda_{\text{QCD}}) = 0$, and is given in terms of the roots of Bessel functions: $\mathcal{M}_{L,k} = \beta_{L,k} \Lambda_{\text{QCD}}$. Upon the substitution $\Phi(\zeta) \sim \zeta^{3/2} \phi(\zeta)$, $\zeta \rightarrow z$ we find

$$[z^2 \partial_z^2 - 3z \partial_z + z^2 \mathcal{M}^2 - (\mu R)^2] \Phi_J = 0, \tag{17}$$

the wave equation which describes the propagation of a scalar mode in a fixed AdS₅ background with AdS radius R . The five dimensional mass μ is related to the orbital angular momentum of the hadronic bound state by $(\mu R)^2 = -4 + L^2$. The quantum mechanical stability $L^2 > 0$ is thus equivalent to the Breitenlohner–Freedman stability bound in AdS [80]. The scaling dimensions are $\Delta = 2 + L$ independent of J in agreement with the twist scaling dimension of a two parton bound state in QCD. Higher spin- J wave equations are obtained by shifting dimensions: $\Phi_J(z) = (z/R)^{-J} \Phi(z)$ [1].

The hard-wall LF model discussed here is equivalent to the hard wall model of Ref. [36]. The variable ζ , $0 \leq \zeta \leq \Lambda_{\text{QCD}}^{-1}$, represents the invariable separation between pointlike constituents and is also the holographic variable z in AdS, thus we can identify $\zeta = z$. Likewise a two-dimensional oscillator with effective potential $U(z) = \kappa^4 z^2 + 2\kappa^2(L + S - 1)$ is similar to the soft-wall model of Ref. [37] which reproduce the usual linear Regge trajectories, where L is the internal orbital angular momentum and S is the internal spin. The soft-wall discussed here correspond to a positive sign dilaton and higher-spin solutions also follow from shifting dimensions: $\Phi_J(z) = (z/R)^{-J} \Phi(z)$ [3].

Individual hadron states can be identified by their interpolating operator at $z \rightarrow 0$. For example, the pseudoscalar meson interpolating operator $\mathcal{O}_{2+L} = \bar{q} \gamma_5 D_{\{\ell_1 \dots \ell_m\}} q$, written in terms of the symmetrized product of covariant derivatives D with total internal orbital momentum $L = \sum_{i=1}^m \ell_i$, is a twist-two, dimension $3 + L$ operator with scaling behavior determined by its twist-dimension $2 + L$. Likewise the vector-meson operator $\mathcal{O}_{2+L}^\mu = \bar{q} \gamma^\mu D_{\{\ell_1 \dots \ell_m\}} q$ has scaling dimension $\Delta = 2 + L$. The scaling behavior of the scalar and vector AdS modes $\Phi(z) \sim z^\Delta$ at $z \rightarrow 0$ is precisely the scaling required to match the scaling dimension of the local pseudoscalar

and vector-meson interpolating operators. The spectral predictions for the light pseudoscalar and vector-mesons in the Chew–Frautschi plot in Fig. 1 and 2 for the soft-wall model discussed here are in good agreement for the principal and daughter Regge trajectories. Radial excitations correspond to the nodes of the wavefunction.

9. Baryons in light-front holography

For baryons, the light-front wave equation is a linear equation determined by the LF transformation properties of spin 1/2 states. A linear confining potential $U(\zeta) \sim \kappa^2 \zeta$ in the LF Dirac equation leads to linear Regge trajectories [79]. For fermionic modes the light-front matrix Hamiltonian eigenvalue equation $D_{\text{LF}}|\psi\rangle = \mathcal{M}|\psi\rangle$, $H_{\text{LF}} = D_{\text{LF}}^2$, in a 2×2 spinor component representation is equivalent to the system of coupled linear equations

$$\begin{aligned} -\frac{d}{d\zeta}\psi_- - \frac{\nu + \frac{1}{2}}{\zeta}\psi_- - \kappa^2\zeta\psi_- &= \mathcal{M}\psi_+, \\ \frac{d}{d\zeta}\psi_+ - \frac{\nu + \frac{1}{2}}{\zeta}\psi_+ - \kappa^2\zeta\psi_+ &= \mathcal{M}\psi_-, \end{aligned} \quad (18)$$

with eigenfunctions

$$\begin{aligned} \psi_+(\zeta) &\sim z^{\frac{1}{2}+\nu} e^{-\kappa^2\zeta^2/2} L_n^\nu(\kappa^2\zeta^2), \\ \psi_-(\zeta) &\sim z^{\frac{3}{2}+\nu} e^{-\kappa^2\zeta^2/2} L_n^{\nu+1}(\kappa^2\zeta^2), \end{aligned} \quad (19)$$

and eigenvalues

$$\mathcal{M}^2 = 4\kappa^2(n + \nu + 1). \quad (20)$$

The baryon interpolating operator $\mathcal{O}_{3+L} = \psi D_{\{\ell_1 \dots \ell_q\}} \psi D_{\ell_{q+1}} \dots D_{\ell_m} \psi$, $L = \sum_{i=1}^m \ell_i$ is a twist 3, dimension $9/2 + L$ with scaling behavior given by its twist-dimension $3 + L$. We thus require $\nu = L + 1$ to match the short distance scaling behavior. Higher spin fermionic modes are obtained by shifting dimensions for the fields as in the bosonic case. Thus, as in the meson sector, the increase in the mass squared for higher baryonic state is $\Delta n = 4\kappa^2$, $\Delta L = 4\kappa^2$ and $\Delta S = 2\kappa^2$, relative to the lowest ground state, the proton. Since our starting point to find the bound state equation of motion for baryons is the light-front, we fix the overall energy scale identical for mesons and baryons by imposing chiral symmetry to the pion [76] in the LF Hamiltonian equations. By contrast, if we start with a five-dimensional action for a scalar field in presence of a positive sign dilaton, the pion is automatically massless.

The predictions for the **56**-plet of light baryons under the SU(6) flavor group are shown in Fig. 5. As for the predictions for mesons in Fig. 2, only confirmed PDG [7] states are shown. The Roper state $N(1440)$ and the

$N(1710)$ are well accounted for in this model as the first and second radial states. Likewise the $\Delta(1660)$ corresponds to the first radial state of the Δ family. The model is successful in explaining the important parity degeneracy observed in the light baryon spectrum, such as the $L=2$, $N(1680) - N(1720)$ degenerate pair and the $L=2$, $\Delta(1905)$, $\Delta(1910)$, $\Delta(1920)$, $\Delta(1950)$ states which are degenerate within error bars. Parity degeneracy of baryons is also a property of the hard wall model, but radial states are not well described in this model [51].

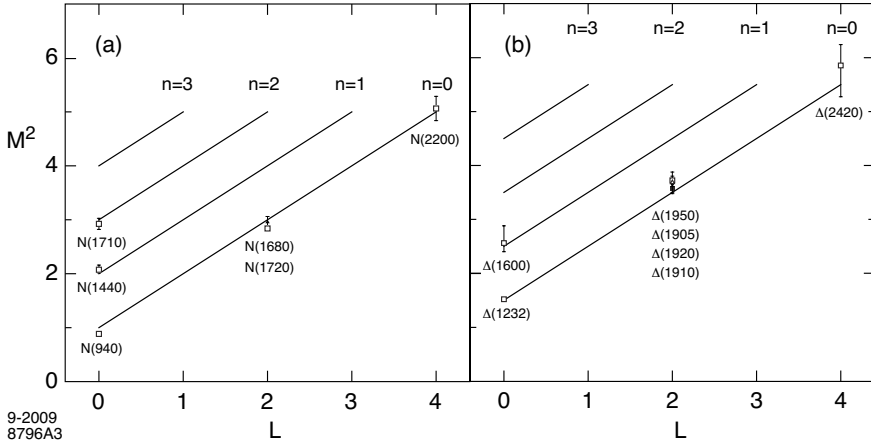


Fig. 5. **56** Regge trajectories for the N and Δ baryon families for $\kappa = 0.5$ GeV.

10. Realization of chiral invariance in light front holography

The proton eigenstate in light-front holography with massless quarks

$$\psi(\zeta) = \psi_+(\zeta)u_+ + \psi_-(\zeta)u_- \tag{21}$$

has $L^z = 0$ and $L^z = +1$ orbital components combined with spin components $S^z = +1/2$ and $S^z = -1/2$, respectively. The four-dimensional spinors u_{\pm} are chiral spinors: $\gamma_5 u_{\pm} = \pm u_{\pm}$. The light-front Fock components ψ_+ and ψ_- have equal probability

$$\int d\zeta |\psi_+(\zeta)|^2 = \int d\zeta |\psi_-(\zeta)|^2, \tag{22}$$

a manifestation of the chiral invariance of the theory for massless quarks. As the equality expressed in (22) follows from integrating the square of the wavefunction for all values of the holographic variable, *i.e.*, over all scales, it is a global property of the theory. On the other hand, for a given scale (a given value of the z or ζ) the solution is not chiral invariant as plus and

minus components have different twist, thus different ζ behavior. At the AdS boundary, $z \rightarrow 0$ or $\zeta \rightarrow 0$, the solution is trivially chiral symmetric since $\psi_+(\zeta) \rightarrow 0$ and $\psi_-(\zeta) \rightarrow 0$ as $\zeta \rightarrow 0$. However, as we go to finite values of z (or ζ) — measuring the proton at different scales — both components plus and minus evolve differently, thus giving locally (for a given scale) chiral symmetry breaking effects, even for massless quarks. The measure of CSB depends in the scale κ or Λ_{QCD} . Chiral symmetry invariance is thus manifest as a global property, and non-perturbative chiral symmetry breaking effects arise locally for AdS theories dual to confining gauge theories, even in the absence of quark masses.

11. The phenomenology of exclusive processes

Exclusive processes play a key role in quantum chromodynamics, testing the primary quark and gluon interactions of QCD and the structure of hadrons at the amplitude level. Two basic pictures have emerged based on perturbative QCD (pQCD) and nonperturbative AdS/QCD. In pQCD hard scattering amplitudes at a high scale $Q^2 \gg \Lambda_{\text{QCD}}^2$ factorize as a convolution of gauge-invariant hadron distribution amplitudes $\phi_H(x_i, Q)$ with the underlying hard scattering quark–gluon subprocess amplitude T_H . The leading power fall-off of the hard scattering amplitude follows from the conformal scaling of the underlying hard-scattering amplitude: $T_H \sim 1/Q^{n-4}$, where n is the total number of fields (quarks, leptons, or gauge fields) participating in the hard scattering [81, 82]. Thus the reaction is dominated by subprocesses and Fock states involving the minimum number of interacting fields. In the case of $2 \rightarrow 2$ scattering processes, this implies the dimensional counting rules $d\sigma/dt(AB \rightarrow CD) = F_{AB \rightarrow CD}(t/s)/s^{n-2}$, where $n = N_A + N_B + N_C + N_D$ and N_H is the minimum number of constituents of H . The result is modified by the ERBL evolution [70, 71] of the distribution amplitudes and the running of the QCD coupling

It is striking that the dimensional counting rules are also a key feature of nonperturbative AdS/QCD models [36]. Although the mechanisms are different, both the pQCD and AdS/QCD approaches depend on the leading twist interpolating operators of the hadron and their structure at short distances. In both theories, hadronic form factors at high Q^2 are dominated by the wavefunctions at small impact separation. This in turn leads to the color transparency phenomena [83, 84]. For example, measurements of pion photoproduction are consistent with dimensional counting $s^7 d\sigma/dt(\gamma p \rightarrow \pi^+ n) \sim \text{constant}$ at fixed CM angle for $s > 7$ GeV. The angular distributions seen in hard large CM angle scattering reactions are consistent with quark interchange, [85] a result also predicted by the hard wall AdS/QCD model. Reviews are given in Refs. [86] and [87]. One sees the onset of perturbative QCD scaling behavior even for exclusive nuclear amplitudes such as deuteron photodisintegration (here $n = 1 + 6 + 3 + 3 = 13$) and $s^{11} d\sigma/dt(\gamma d \rightarrow pn) \sim \text{constant}$ at fixed CM angle [88–90]. The measured deuteron form factor [91]

also appears to follow the leading-twist QCD predictions [92] at large momentum transfers in the few GeV region. The six color-triplet quarks of the valence Fock state of the deuteron can be arranged as a sum of five different color-singlet states, only one of which can be identified with the neutron-proton state and can account for the large magnitude of the deuteron form factor at high scales. A measurement of $d\sigma/dt(\gamma d \rightarrow \Delta^{++}\Delta)$ in the scaling region can establish the role of “hidden-color” degrees of freedom [93] of the nuclear wavefunction in hard deuteron reactions.

In the case of pQCD, the near-constancy of the effective QCD coupling at small scales helps explain the general empirical success of the dimensional counting rules for the near-conformal power law fall-off of form factors and fixed-angle scaling [94].

Color transparency [83, 84] is a key property of color gauge theory, and it thus stands at the foundations of QCD. Color transparency has been confirmed in diffractive dijet production, [95] pion photoproduction [96] and vector-meson electroproduction, [97] but it is very important to also systematically validate it in large-angle hadron scattering processes. Color transparency and higher-twist subprocesses [98–102], where the trigger hadron is produced directly, such as $uu \rightarrow p\bar{d}$, can account for the anomalous growth of the baryon-to-meson ratio with increasing centrality observed in heavy ion collisions at RHIC [103].

12. Anomalies in exclusive processes

Some exceptions to the general success of dimensional counting are known.

The transition form factor $F(Q^2)_{\gamma \rightarrow \pi^0}$ between a real photon and a pion has been measured at BaBar to high $Q^2 \simeq 10 \text{ GeV}^2$, falling at high photon virtuality roughly as $1/Q^{3/2}$ rather than the predicted $1/Q^2$ fall-off. In contrast, preliminary measurements from BaBar [104] indicate that the transition form factors $F(Q^2)_{\gamma \rightarrow \eta}$ and $F(Q^2)_{\gamma \rightarrow \eta'}$ are consistent with the pQCD expectations. The photon to meson transition form factor is the simplest QCD hadronic exclusive amplitude, and thus it is critical to understand this discrepancy. As we shall discuss below, AdS/QCD predicts a broad distribution amplitude $\phi_\pi(x, Q)$ in the nonperturbative domain, but since ERBL evolution leads to a narrower distribution in the high Q domain, it cannot explain the BaBar anomaly. It is difficult to imagine that the pion distribution amplitude is close to flat [105–108] since this corresponds to a pointlike non-composite hadron. It is crucial to measure $d\sigma/dt(\gamma\gamma \rightarrow \pi^0\pi^0)$ since the CM angular distribution is very sensitive to the shape of $\phi_\pi(x, Q)$ [109].

The Hall A Collaboration [110] at JLab has reported another significant exception to the general empirical success of dimensional counting in fixed-CM-angle Compton scattering $d\sigma/dt(\gamma p \rightarrow \gamma p) \sim F(\theta_{\text{CM}})/s^8$ instead of the predicted $1/s^6$ scaling. The deviations from fixed-angle conformal

scaling may be due to corrections from resonance contributions in the JLab energy range. It is interesting that the hadron form factor $R_V(t)$ [111] which multiplies the $\gamma q \rightarrow \gamma q$ amplitude is found by Hall A to scale as $1/t^2$, in agreement with the pQCD and AdS/QCD prediction. In addition, the Belle measurement [112] of the timelike two-photon cross-section $d\sigma/dt(\gamma\gamma \rightarrow p\bar{p})$ is consistent with $1/s^6$ scaling.

Although large-angle proton–proton elastic scattering is well described by dimensional scaling $s^{10}d\sigma/dt(pp \rightarrow pp) \sim \text{constant}$ at fixed CM angle, extraordinarily large spin–spin correlations are observed [113]. The ratio of scattering cross-sections for spin-parallel and normal to the scattering plane *versus* spin-antiparallel reaches $R_{NN} \simeq 4$ in large angle $pp \rightarrow pp$ at $\sqrt{s} \simeq 5$ GeV; this is a remarkable example of “exclusive transversity”. Color transparency is observed at lower energies but it fails [114] at the same energy, where R_{NN} becomes large. In fact, these anomalies have a natural explanation [115] as a resonance effect related to the charm threshold in pp scattering. Alternative explanations of the large spin correlation are discussed and reviewed in Ref. [116]. Resonance formation is a natural phenomenon when all constituents are relatively at rest. For example, a resonance effect can occur due to the intermediate state $uud\bar{u}d\bar{c}\bar{c}$ at the charm threshold $\sqrt{s} = 5$ GeV in pp collisions. Since the c and \bar{c} have opposite intrinsic parity, the resonance appears in the $L = J = S = 1$ partial wave for $pp \rightarrow pp$ which is only allowed for spin-parallel and normal to the scattering plane $A_{NN} = 1$ [115]. Resonance formation at the charm threshold also explains the dramatic quenching of color transparency seen in quasielastic pn scattering by the EVA BNL experiment [114] in the same kinematic region. The reason why these effects are apparent in $pp \rightarrow pp$ scattering is that the amplitude for the formation of an $uud\bar{u}d\bar{c}\bar{c}$ s -channel resonance in the intermediate state is of the same magnitude as the fast-falling background $pp \rightarrow pp$ pQCD amplitude from quark interchange at large CM angles: $M(pp \rightarrow pp) \sim 1/u^2t^2$. The open charm cross-section in pp scattering is predicted by unitarity to be of the order of $1 \mu\text{b}$ at threshold [115]. One also expects similar novel QCD phenomena in large-angle photoproduction $\gamma p \rightarrow \pi N$ near the charm threshold, including the breakdown of color transparency and strong spin–spin correlations. These effects can be tested by measurements at the new JLab 12 GeV facility, which would confirm resonance formation in a low partial wave in $\gamma p \rightarrow \pi N$ at $\sqrt{s} \simeq 4$ GeV due to attractive forces in the $uud\bar{c}\bar{c}$ channel.

Another difficulty for the application of pQCD to exclusive processes is the famous $J/\psi \rightarrow \rho\pi$ puzzle; the observed unusually large branching ratio for $J/\psi \rightarrow \rho\pi$. In contrast, the branching ratio for $\Psi' \rightarrow \rho\pi$ is very small. Such decays into pseudoscalar plus vector mesons require light-quark helicity suppression or internal orbital angular momentum and thus should be suppressed by hadron helicity conservation in pQCD. However, the $J/\psi \rightarrow \rho\pi$ puzzle can be explained by the presence of intrinsic charm Fock states in the outgoing mesons [117].

13. Nucleon form factor in light-front holography

As an example of the scaling behavior of a twist $\tau = 3$ hadron, we compute the spin non-flip nucleon form factor in the soft wall model [79]. The proton and neutron Dirac form factors are given by

$$F_1^p(Q^2) = \int d\zeta J(Q, \zeta) |\psi_+(\zeta)|^2, \tag{23}$$

$$F_1^n(Q^2) = -\frac{1}{3} \int d\zeta J(Q, \zeta) [|\psi_+(\zeta)|^2 - |\psi_-(\zeta)|^2], \tag{24}$$

where $F_1^p(0) = 1$, $F_1^n(0) = 0$. The non-normalizable mode $J(Q, z)$ is the solution of the AdS wave equation for the external electromagnetic current in presence of a dilaton background $\exp(\pm\kappa^2 z^2)$ [46, 118]. Plus and minus components of the twist 3 nucleon LFWF are

$$\psi_+(\zeta) = \sqrt{2}\kappa^2 \zeta^{3/2} e^{-\kappa^2 \zeta^2/2}, \quad \Psi_-(\zeta) = \kappa^3 \zeta^{5/2} e^{-\kappa^2 \zeta^2/2}. \tag{25}$$

The results for $Q^4 F_1^p(Q^2)$ and $Q^4 F_1^n(Q^2)$ and are shown in Fig. 6.

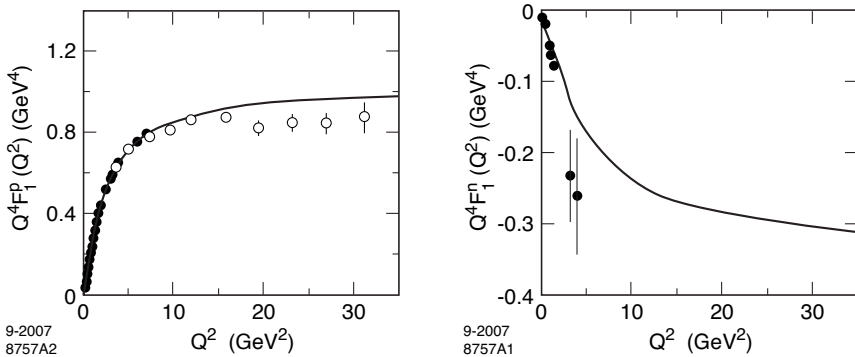


Fig. 6. Predictions for $Q^4 F_1^p(Q^2)$ and $Q^4 F_1^n(Q^2)$ in the soft wall model for $\kappa = 0.424$ GeV [119].

14. Nonperturbative running coupling from light-front holography

The concept of a running coupling $\alpha_s(Q^2)$ in QCD is usually restricted to the perturbative domain. However, as in QED, it is useful to define the coupling as an analytic function valid over the full space-like and time-like domains. The study of the non-Abelian QCD coupling at small momentum transfer is a complex problem because of gluonic self-coupling and color confinement.

The definition of the running coupling in perturbative quantum field theory is scheme-dependent. As discussed by Grunberg, [120] an effective coupling or charge can be defined directly from physical observables. Effective charges defined from different observables can be related to each other in the leading-twist domain using commensurate scale relations (CSR) [121]. The potential between infinitely heavy quarks can be defined analytically in momentum transfer space as the product of the running coupling times the Born gluon propagator: $V(q) = -4\pi C_F \alpha_V(q)/q^2$. This effective charge defines a renormalization scheme — the α_V scheme of Appelquist, Dine, and Muzinich [122]. In fact, the holographic coupling $\alpha_s^{\text{AdS}}(Q^2)$ can be considered to be the nonperturbative extension of the α_V effective charge defined in Ref. [122]. We can also make use of the g_1 scheme, where the strong coupling $\alpha_{g_1}(Q^2)$ is determined from the Bjorken sum rule [123]. The coupling $\alpha_{g_1}(Q^2)$ has the advantage that it is the best-measured effective charge, and it can be used to extrapolate the definition of the effective coupling to large distances [124]. Since α_{g_1} has been measured at intermediate energies, it is particularly useful for studying the transition from small to large distances.

We have also shown [125] how the LF holographic mapping of effective classical gravity in AdS space, modified by a positive-sign dilaton background, can be used to identify an analytically simple color-confining non-perturbative effective coupling $\alpha_s^{\text{AdS}}(Q^2)$ as a function of the space-like momentum transfer $Q^2 = -q^2$. This coupling incorporates confinement and agrees well with effective charge observables and lattice simulations. It also exhibits an infrared fixed point at small Q^2 and asymptotic freedom at large Q^2 . However, the fall-off of $\alpha_s^{\text{AdS}}(Q^2)$ at large Q^2 is exponential: $\alpha_s^{\text{AdS}}(Q^2) \sim e^{-Q^2/\kappa^2}$, rather than the pQCD logarithmic fall-off. It agrees with hadron physics data extracted phenomenologically from different observables, as well as with the predictions of models with built-in confinement and lattice simulations. We also show that a phenomenological extended coupling can be defined which implements the pQCD behavior. The β -function derived from light-front holography becomes significantly negative in the non-perturbative regime $Q^2 \sim \kappa^2$, where it reaches a minimum, signaling the transition region from the infrared (IR) conformal region, characterized by hadronic degrees of freedom, to a pQCD conformal ultraviolet (UV) regime where the relevant degrees of freedom are the quark and gluon constituents. The β -function vanishes at large Q^2 consistent with asymptotic freedom, and it vanishes at small Q^2 consistent with an infrared fixed point [55, 126].

Let us consider a five-dimensional gauge field F propagating in AdS_5 space in presence of a dilaton background $\varphi(z)$ which introduces the energy scale κ in the five-dimensional action. At quadratic order in the field strength the action is

$$S = -\frac{1}{4} \int d^5x \sqrt{g} e^{\varphi(z)} \frac{1}{g_5^2} F^2, \quad (26)$$

where the metric determinant of AdS₅ is $\sqrt{g} = (R/z)^5$, $\varphi = \kappa^2 z^2$ and the square of the coupling g_5 has dimensions of length. We can identify the prefactor

$$g_5^{-2}(z) = e^{\varphi(z)} g_5^{-2} \tag{27}$$

in the AdS action (26) as the effective coupling of the theory at the length scale z . The coupling $g_5(z)$ then incorporates the non-conformal dynamics of confinement. The five-dimensional coupling $g_5(z)$ is mapped, modulo a constant, into the Yang–Mills (YM) coupling g_{YM} of the confining theory in physical space-time using light-front holography. One identifies z with the invariant impact separation variable ζ which appears in the LF Hamiltonian: $g_5(z) \rightarrow g_{\text{YM}}(\zeta)$. Thus

$$\alpha^{\text{AdS}}(\zeta) = \frac{g_{\text{YM}}^2(\zeta)}{4\pi} \propto e^{-\kappa^2 \zeta^2}. \tag{28}$$

In contrast with the 3-dimensional radial coordinates of the non-relativistic Schrödinger theory, the natural light-front variables are the two-dimensional cylindrical coordinates (ζ, ϕ) and the light-cone fraction x . The physical coupling measured at the scale Q is the two-dimensional Fourier transform of the LF transverse coupling $\alpha_s^{\text{AdS}}(\zeta)$ (28). Integration over the azimuthal angle ϕ gives the Bessel transform

$$\alpha_s^{\text{AdS}}(Q^2) \sim \int_0^\infty \zeta d\zeta J_0(\zeta Q) \alpha_s^{\text{AdS}}(\zeta) \tag{29}$$

in the $q^+ = 0$ light-front frame where $Q^2 = -q^2 = -\mathbf{q}_\perp^2 > 0$ is the square of the space-like four-momentum transferred to the hadronic bound state. Using this ansatz we then have from Eq. (29)

$$\alpha_s^{\text{AdS}}(Q^2) = \alpha_s^{\text{AdS}}(0) e^{-Q^2/4\kappa^2}. \tag{30}$$

In contrast, the negative dilaton solution $\varphi = -\kappa^2 z^2$ leads to an integral which diverges at large ζ . We identify $\alpha_s^{\text{AdS}}(Q^2)$ with the physical QCD running coupling in its nonperturbative domain.

The flow equation (27) from the scale dependent measure for the gauge fields can be understood as a consequence of field-strength renormalization. In physical QCD we can rescale the non-Abelian gluon field $A^\mu \rightarrow \lambda A^\mu$ and field strength $G^{\mu\nu} \rightarrow \lambda G^{\mu\nu}$ in the QCD Lagrangian density \mathcal{L}_{QCD} by a compensating rescaling of the coupling strength $g \rightarrow \lambda^{-1}g$. The renormalization of the coupling $g_{\text{phys}} = Z_3^{1/2} g_0$, where g_0 is the bare coupling in the Lagrangian in the UV-regulated theory, is thus equivalent to the renormalization of the vector potential and field strength: $A_{\text{ren}}^\mu = Z_3^{-1/2} A_0^\mu$, $G_{\text{ren}}^{\mu\nu} = Z_3^{-1/2} G_0^{\mu\nu}$ with a rescaled Lagrangian density $\mathcal{L}_{\text{QCD}}^{\text{ren}} = Z_3^{-1} \mathcal{L}_{\text{QCD}}^0 =$

$(g_{\text{phys}}/g_0)^{-2}\mathcal{L}_0$. In lattice gauge theory, the lattice spacing a serves as the UV regulator, and the renormalized QCD coupling is determined from the normalization of the gluon field strength as it appears in the gluon propagator. The inverse of the lattice size L sets the mass scale of the resulting running coupling. As is the case in lattice gauge theory, color confinement in AdS/QCD reflects nonperturbative dynamics at large distances. The QCD couplings defined from lattice gauge theory and the soft wall holographic model are thus similar in concept, and both schemes are expected to have similar properties in the nonperturbative domain, up to a rescaling of their respective momentum scales.

14.1. Comparison of the holographic coupling with other effective charges

The effective coupling $\alpha^{\text{AdS}}(Q^2)$ (solid line) is compared in Fig. 7 with experimental and lattice data. For this comparison to be meaningful, we have to impose the same normalization on the AdS coupling as the g_1 coupling. This defines α_s^{AdS} normalized to the g_1 scheme: $\alpha_{g_1}^{\text{AdS}}(Q^2=0) = \pi$. Details on the comparison with other effective charges are given in Ref. [54].

The couplings in Fig. 7 (top) agree well in the strong coupling regime up to $Q \sim 1$ GeV. The value $\kappa = 0.54$ GeV is determined from the vector-meson Regge trajectory [3]. The lattice results shown in Fig. 7 from Ref. [52] have been scaled to match the perturbative UV domain. The effective charge α_{g_1} has been determined in Ref. [54] from several experiments. Fig. 7 also displays other couplings from different observables as well as α_{g_1} which is computed from the Bjorken sum rule [123] over a large range of momentum transfer (grey/cyan band). A recent analysis [127] using the pinch scheme [126] predicts a similar fixed-point behavior.

At $Q^2=0$ one has the constraint on the slope of α_{g_1} from the Gerasimov–Drell–Hearn (GDH) sum rule [128] which is also shown in the figure. The results show no sign of a phase transition, cusp, or other non-analytical behavior, a fact which allows us to extend the functional dependence of the coupling to large distances. As discussed below, the smooth behavior of the AdS strong coupling also allows us to extrapolate its form to the perturbative domain [125].

The hadronic model obtained from the dilaton-modified AdS space provides a semiclassical first approximation to QCD. Color confinement is introduced by the harmonic oscillator potential, but effects from gluon creation and absorption are not included in this effective theory. The nonperturbative confining effects vanish exponentially at large momentum transfer (Eq. (30)), and thus the logarithmic fall-off from pQCD quantum loops will dominate in this regime. The running coupling α_s^{AdS} given by Eq. (30) is obtained from a color-confining potential. Since the strong coupling is an analytical function of the momentum transfer at all scales, we can extend the range of applicability of α_s^{AdS} by matching to a perturbative coupling at the transition scale $Q \sim 1$ GeV, where pQCD contributions become important,

as described in Ref. [125]. The smoothly extrapolated result (dot-dashed line) for α_s is also shown in Fig. 7. In order to have a fully analytical model, we write

$$\alpha_{\text{Modified},g_1}^{\text{AdS}}(Q^2) = \alpha_{g_1}^{\text{AdS}}(Q^2) g_+(Q^2) + \alpha_{g_1}^{\text{fit}}(Q^2) g_-(Q^2), \quad (31)$$

where $g_{\pm}(Q^2) = 1/(1 + e^{\pm(Q^2 - Q_0^2)/\tau^2})$ are smeared step functions which match the two regimes. The parameter τ represents the width of the transition region. Here $\alpha_{g_1}^{\text{AdS}}$ is given by Eq. (30) with the normalization $\alpha_{g_1}^{\text{AdS}}(0) = \pi$ — the plain black line in Fig. 7 — and $\alpha_{g_1}^{\text{fit}}$ in Eq. (31) is the analytical fit to the measured coupling α_{g_1} [54]. The couplings are chosen to have the same normalization at $Q^2 = 0$. The smoothly extrapolated result (dot-dashed line) for α_s is also shown in Fig. 7. We use the parameters $Q_0^2 = 0.8 \text{ GeV}^2$ and $\tau^2 = 0.3 \text{ GeV}^2$.

14.2. The β -function from AdS/QCD

The β -function for the nonperturbative effective coupling obtained from the LF holographic mapping in a positive dilaton modified AdS background is

$$\beta^{\text{AdS}}(Q^2) = \frac{d}{d \log Q^2} \alpha^{\text{AdS}}(Q^2) = -\frac{\pi Q^2}{4\kappa^2} e^{-Q^2/(4\kappa^2)}. \quad (32)$$

The solid line in Fig. 7 (bottom) corresponds to the light-front holographic result Eq. (32). Near $Q_0 \simeq 2\kappa \simeq 1 \text{ GeV}$, we can interpret the results as a transition from the nonperturbative IR domain to the quark and gluon degrees of freedom in the perturbative UV regime. The transition momentum scale Q_0 is compatible with the momentum transfer for the onset of scaling behavior in exclusive reactions where quark counting rules are observed [81]. For example, in deuteron photo-disintegration the onset of scaling corresponds to momentum transfer of 1.0 GeV to the nucleon involved [129]. Dimensional counting is built into the AdS/QCD soft and hard wall models since the AdS amplitudes $\Phi(z)$ are governed by their twist scaling behavior z^τ at short distances, $z \rightarrow 0$ [36].

Also shown in Fig. 7 (bottom) are the β -functions obtained from phenomenology and lattice calculations. For clarity, we present only the LF holographic predictions, the lattice results from [52] and the experimental data supplemented by the relevant sum rules. The dot-dashed curve corresponds to the extrapolated approximation obtained by matching to AdS results to the perturbative coupling [125] given by Eq. (31). The β -function extracted from LF holography, as well as the forms obtained from the works of Cornwall [126], Bloch, Fisher *et al.* [130], Burkert and Ioffe [131], and Furui and Nakajima [52] are seen to have a similar shape and magnitude.

Judging from these results, we infer that the actual β -function of QCD will extrapolate between the non-perturbative results for $Q < 1$ GeV and the pQCD results for $Q > 1$ GeV. We also observe that the general conditions

$$\beta(Q \rightarrow 0) = \beta(Q \rightarrow \infty) = 0, \quad (33)$$

$$\beta(Q) < 0 \quad \text{for } Q > 0, \quad (34)$$

$$\left. \frac{d\beta}{dQ} \right|_{Q=Q_0} = 0, \quad (35)$$

$$\left. \frac{d\beta}{dQ} \right|_{Q < Q_0} < 0, \quad \left. \frac{d\beta}{dQ} \right|_{Q > Q_0} > 0 \quad (36)$$

are satisfied by our model β -function obtained from LF holography.

Eq. (33) expresses the fact that QCD approaches a conformal theory in both the far ultraviolet and deep infrared regions. In the semiclassical approximation to QCD without particle creation or absorption, the β -function is zero and the approximate theory is scale invariant in the limit of massless quarks [132]. When quantum corrections are included, the conformal behavior is preserved at very large Q because of asymptotic freedom and near $Q \rightarrow 0$ because the theory develops a fixed point. An infrared fixed point is in fact a natural consequence of color confinement [126]: since the propagators of the colored fields have a maximum wavelength, all loop integrals in the computation of the gluon self-energy decouple at $Q^2 \rightarrow 0$ [55]. Condition (34) for Q^2 large, expresses the basic anti-screening behavior of QCD where the strong coupling vanishes. The β -function in QCD is essentially negative, thus the coupling increases monotonically from the UV to the IR where it reaches its maximum value: it has a finite value for a theory with a mass gap. Equation (35) defines the transition region at Q_0 where the β -function has a minimum. Since there is only one hadronic-partonic transition, the minimum is an absolute minimum; thus the additional conditions expressed in Eq. (36) follow immediately from Eqs. (33)–(35). The conditions given by Eqs. (33)–(36) describe the essential behavior of the full β -function for an effective QCD coupling whose scheme/definition is similar to that of the V-scheme.

15. Vacuum effects and light-front quantization

The LF vacuum is remarkably simple in light-cone quantization because of the restriction $k^+ \geq 0$. For example in QED, vacuum graphs such as $e^+e^-\gamma$ associated with the zero-point energy do not arise. In the Higgs theory, the usual Higgs vacuum expectation value is replaced with a $k^+ = 0$ zero mode [62]; however, the resulting phenomenology is identical to the standard analysis.

Hadronic condensates play an important role in quantum chromodynamics. It is widely held that quark and gluon vacuum condensates have a physical existence, independent of hadrons, measurable spacetime-independent configurations of QCD's elementary degrees-of-freedom in a hadron-less

ground state. However, a non-zero spacetime-independent QCD vacuum condensate poses a critical dilemma for gravitational interactions because it would lead to a cosmological constant some 45 orders of magnitude larger than observation. As noted in Ref. [61], this conflict is avoided if strong interaction condensates are properties of the light-front wavefunctions of the hadrons, rather than the hadron-less ground state of QCD.

The usual assumption that non-zero vacuum condensates exist and possess a measurable reality has long been recognized as posing a conundrum for the light-front formulation of QCD. In the light-front formulation, the ground-state is a structureless Fock space vacuum, in which case it would seem to follow that dynamical chiral symmetry breaking (CSB) is impossible. In fact, as first argued by Casher and Susskind [60] dynamical CSB must be a property of hadron wavefunctions, not of the vacuum in the light-front framework. This thesis has also been explored in a series of recent articles [31, 55, 61].

Conventionally, the quark and gluon condensates are considered to be properties of the QCD vacuum and hence to be constant throughout spacetime. A new perspective on the nature of QCD condensates $\langle \bar{q}q \rangle$ and $\langle G_{\mu\nu}G^{\mu\nu} \rangle$, particularly where they have spatial and temporal support, has recently been presented [55, 61, 133, 134]. Their spatial support is restricted to the interior of hadrons, since these condensates arise due to the interactions of quarks and gluons which are confined within hadrons.

For example, consider a meson consisting of a light quark q bound to a heavy antiquark, such as a B meson. One can analyze the propagation of the light q in the background field of the heavy \bar{b} quark. Solving the Dyson–Schwinger equation for the light quark one obtains a non-zero dynamical mass and, via the connection mentioned above, hence a non-zero value of the condensate $\langle \bar{q}q \rangle$. But this is not a true vacuum expectation value; instead, it is the matrix element of the operator $\bar{q}q$ in the background field of the \bar{b} quark. The change in the (dynamical) mass of the light quark in this bound state is somewhat reminiscent of the energy shift of an electron in the Lamb shift, in that both are consequences of the fermion being in a bound state rather than propagating freely. Similarly, it is important to use the equations of motion for confined quarks and gluon fields when analyzing current correlators in QCD, not free propagators, as has often been done in traditional analyses of operator products. Since the distance between the quark and antiquark cannot become arbitrarily large, one cannot create a quark condensate which has uniform extent throughout the universe. Thus in a fully self-consistent treatment of the bound state, this phenomenon occurs in the background field of the \bar{b} -quark, whose influence on light-quark propagation is primarily concentrated in the far infrared and whose presence ensures the manifestations of light-quark dressing are gauge invariant.

In the case of the pion one finds that the vacuum quark condensate that appears in the Gell-Mann–Oakes–Renner formula, is, in fact, a chiral-limit value of an “in-pion” condensate. This condensate is no more a property of

the “vacuum” than the pion’s chiral-limit leptonic decay constant. One can connect the Bethe–Salpeter formalism to the light-front formalism, by fixing the light-front time τ . This then leads to the Fock state expansion. In fact, dynamical CSB in the light-front formulation, expressed via “in-hadron” condensates, can be shown to be connected with sea-quarks derived from higher Fock states. This solution is similar to that discussed in Ref. [60]. Moreover, Ref. [135] establishes the equivalence of all three definitions of the vacuum quark condensate: a constant in the operator product expansion [136, 137] via the Banks–Casher formula [138] and the trace of the chiral-limit dressed-quark propagator.

AdS/QCD also provides a description of chiral symmetry breaking by using the propagation of a scalar field $X(z)$ which encodes the coupling of the quark mass m_q and quark condensate $\langle \bar{q}q \rangle$ to the hadron. In the hard-wall model the AdS solution has the form [48, 49]

$$X(z) = a_1 z + a_2 z^3, \quad (37)$$

where a_1 is proportional to the current-quark mass and a_2 to the quark condensate $\langle \bar{q}q \rangle$. Since the quark is a color nonsinglet, the propagation of $X(z)$, and thus the domain of the quark condensate, is limited to the region of color confinement. The effect of the a_2 term varies within the hadron. This is consistent with the idea that the effect of CSB increases as one goes toward large interquark separation. In the light-front view, this is due to the higher Fock states. In fact, that the CSB dynamics depends on the total size of the hadron, means that there will be unexpected dependence of the effective quark mass on the spectators. For example, the effect of the u quark mass term will be smaller in a $B^+(\bar{b}u)$ than a $K^+(\bar{s}u)$ since the B has a smaller transverse size [139].

The picture of condensates with spatial support restricted to hadrons is also in general agreement with results from chiral bag models [140–142] which modify the original MIT bag by coupling a pion field to the surface of the bag in a chirally invariant manner. It is important to notice however, that AdS/QCD does not help to elucidate the nature of the in-hadron *versus* vacuum condensates. The quark mass and the condensate are from the point of view of holography, at least in the fixed background approximation, arbitrary constants given by the initial conditions. What is physically relevant from the AdS/QCD perspective is the coupling of m_q and $\langle \bar{q}q \rangle$ to $X(z)$, and this leads to observable effects.

16. Conclusions

The combination of Anti-de Sitter space with light-front holography provides an accurate first approximation for the spectra and wavefunctions of meson and baryon light-quark bound states. This new framework provides an elegant connection between a semiclassical first approximation to QCD,

quantized on the light-front, with hadronic modes propagating on a fixed AdS background. The resulting bound-state Hamiltonian equation of motion in QCD leads to relativistic light-front wave equations in the invariant impact variable ζ , which measures the separation of the quark and gluonic constituents within the hadron at equal light-front time. This corresponds to the effective single-variable relativistic Schrödinger-like equation in the AdS fifth dimension coordinate z , Eq. (1). The eigenvalues give the hadronic spectrum, and the eigenmodes represent the probability distributions of the hadronic constituents at a given scale. In particular, the light-front holographic mapping of effective classical gravity in AdS space, modified by a positive-sign dilaton background, provides a very good description of the spectrum and form factors of light mesons and baryons. We emphasize that the hadron eigenstate generally has components with different orbital angular momentum. For example, the proton eigenstate in AdS/QCD with massless quarks has $L = 0$ and $L = 1$ light-front Fock components with equal probability — a novel manifestation of chiral invariance.

We have also shown that the light-front holographic mapping of effective classical gravity in AdS space, modified by the positive-sign dilaton background predicts the form of a non-perturbative effective coupling $\alpha_s^{\text{AdS}}(Q)$ and its β -function. The AdS/QCD running coupling is in very good agreement with the effective coupling α_{g_1} extracted from the Bjorken sum rule. The holographic β -function displays a transition from nonperturbative to perturbative regimes at a momentum scale $Q \sim 1$ GeV. Our analysis indicates that light-front holography captures the characteristics of the full β -function of QCD and the essential dynamics of confinement, thus giving further support to the application of the gauge/gravity duality to the confining dynamics of strongly coupled QCD.

There are many phenomenological applications where detailed knowledge of the QCD coupling and the renormalized gluon propagator at relatively soft momentum transfer are essential. This includes exclusive and semi-exclusive processes as well as the rescattering interactions which create the leading-twist Sivers single-spin correlations in semi-inclusive deep inelastic scattering [143, 144], the Boer–Mulders functions which lead to anomalous $\cos 2\phi$ contributions to the lepton pair angular distribution in the unpolarized Drell–Yan reaction [145], and the Sommerfeld–Sakharov–Schwinger correction to heavy quark production at threshold [146]. The confining AdS/QCD coupling from light-front holography thus can provide a quantitative understanding of this factorization-breaking physics [147].

A new perspective on the nature of quark and gluon condensates in quantum chromodynamics has also been addressed [55, 133, 134]: the spatial support of QCD condensates is restricted to the interior of hadrons, since they arise due to the interactions of confined quarks and gluons. In LF theory, the condensate physics is replaced by the dynamics of higher non-valence Fock states as shown by Casher and Susskind [60]. In particular, chiral symmetry is broken in a limited domain of size $1/m_\pi$, in analogy to the

limited physical extent of superconductor phases. This novel description of chiral symmetry breaking in terms of “in-hadron condensates” has also been observed in Bethe–Salpeter studies [148,149]. This picture also explains the results of recent studies [150–152] which find no significant signal for the vacuum gluon condensate.

We thank Alexander Deur, Craig Roberts, Robert Shrock, and Peter Tandy for collaborations. This research was supported by the Department of Energy contract DE-AC02-76SF00515. Invited talk, presented by S.J.B. at the L Cracow School, Zakopane, Poland in honor of its founder, Andrzej Białas. G.F.d.T. thanks the members of the High Energy Physics Group at the Imperial College in London for their hospitality. SLAC-PUB-14258.

REFERENCES

- [1] G.F. de Teramond, S.J. Brodsky, *Phys. Rev. Lett.* **102**, 081601 (2009) [arXiv:0809.4899 [hep-ph]].
- [2] P.A.M. Dirac, *Rev. Mod. Phys.* **21**, 392 (1949).
- [3] G.F. de Teramond, S.J. Brodsky, *Nucl. Phys. B, Proc. Suppl.* **199**, 89 (2010) [arXiv:0909.3900 [hep-ph]].
- [4] P. Danielewicz, J.M. Namyslowski, *Phys. Lett.* **B81**, 110 (1979).
- [5] V.A. Karmanov, *Nucl. Phys.* **B166**, 378 (1980).
- [6] S.D. Glazek, *Acta Phys. Pol. B* **15**, 889 (1984).
- [7] C. Amsler *et al.* [Particle Data Group], *Phys. Lett.* **B667**, 1 (2008).
- [8] H. Boschi-Filho, N.R.F. Braga, H.L. Carrion, *Phys. Rev.* **D73**, 047901 (2006) [arXiv:hep-th/0507063].
- [9] N. Evans, A. Tedder, *Phys. Lett.* **B642**, 546 (2006) [arXiv:hep-ph/0609112].
- [10] D.K. Hong, T. Inami, H.U. Yee, *Phys. Lett.* **B646**, 165 (2007) [arXiv:hep-ph/0609270].
- [11] P. Colangelo, F. De Fazio, F. Jugeau, S. Nicotri, *Phys. Lett.* **B652**, 73 (2007) [arXiv:hep-ph/0703316].
- [12] H. Forkel, *Phys. Rev.* **D78**, 025001 (2008) [arXiv:0711.1179 [hep-ph]].
- [13] A. Vega, I. Schmidt, *Phys. Rev.* **D78**, 017703 (2008) [arXiv:0806.2267 [hep-ph]].
- [14] K. Nawa, H. Suganuma, T. Kojo, *Mod. Phys. Lett.* **A23**, 2364 (2008) [arXiv:0806.3040 [hep-th]].
- [15] W. de Paula, T. Frederico, H. Forkel, M. Beyer, *Phys. Rev.* **D79**, 075019 (2009) [arXiv:0806.3830 [hep-ph]].
- [16] P. Colangelo *et al.*, *Phys. Rev.* **D78**, 055009 (2008) [arXiv:0807.1054 [hep-ph]].

- [17] H. Forkel, E. Klempt, *Phys. Lett.* **B679**, 77 (2009) [arXiv:0810.2959 [hep-ph]].
- [18] H.C. Ahn, D.K. Hong, C. Park, S. Siwach, *Phys. Rev.* **D80**, 054001 (2009) [arXiv:0904.3731 [hep-ph]].
- [19] Y.Q. Sui, Y.L. Wu, Z.F. Xie, Y.B. Yang, *Phys. Rev.* **D81**, 014024 (2010) [arXiv:0909.3887 [hep-ph]].
- [20] J.I. Kapusta, T. Springer, *Phys. Rev.* **D81**, 086009 (2010) [arXiv:1001.4799 [hep-ph]].
- [21] P. Zhang, *Phys. Rev.* **D81**, 114029 (2010) [arXiv:1002.4352 [hep-ph]]; *J. High Energy Phys.* **1005**, 039 (2010) [arXiv:1003.0558 [hep-ph]]; arXiv:1007.2163 [hep-ph].
- [22] I. Iatrakis, E. Kiritsis, A. Paredes, *Phys. Rev.* **D81**, 115004 (2010) [arXiv:1003.2377 [hep-ph]].
- [23] W. de Paula, T. Frederico, *Nucl. Phys. Proc. Suppl.* **199**, 113 (2010) [arXiv:1004.1555 [hep-ph]].
- [24] T. Branz *et al.*, arXiv:1008.0268 [hep-ph].
- [25] See also: M. Kirchbach, C.B. Compean, *Phys. Rev.* **D82**, 034008 (2010) [arXiv:1003.1747 [hep-ph]]; S.J. Wang, J. Tao, X.B. Guo, L. Li, arXiv:1007.2462 [hep-th].
- [26] R. Baldini *et al.*, *Eur. Phys. J.* **C11**, 709 (1999).
- [27] V. Tadevosyan *et al.* [Fpi1 Collaboration], *Phys. Rev.* **C75**, 055205 (2007) [arXiv:nucl-ex/0607007].
- [28] T. Horn *et al.* [Fpi2 Collaboration], *Phys. Rev. Lett.* **97**, 192001 (2006) [arXiv:nucl-ex/0607005].
- [29] H.J. Kwee, R.F. Lebed, *J. High Energy Phys.* **0801**, 027 (2008) [arXiv:0708.4054 [hep-ph]]; *Phys. Rev.* **D77**, 115007 (2008) [arXiv:0712.1811 [hep-ph]].
- [30] H.R. Grigoryan, A.V. Radyushkin, *Phys. Rev.* **D76**, 115007 (2007) [arXiv:0709.0500 [hep-ph]]; *Phys. Rev.* **D78**, 115008 (2008) [arXiv:0808.1243 [hep-ph]].
- [31] S.J. Brodsky, G. de Teramond, R. Shrock, *AIP Conf. Proc.* **1056**, 3 (2008) [arXiv:0807.2484 [hep-ph]].
- [32] C.T. Munger, S.J. Brodsky, I. Schmidt, *Phys. Rev.* **D49**, 3228 (1994).
- [33] J.P. Vary *et al.*, arXiv:0905.1411 [nucl-th].
- [34] A. Deur, V. Burkert, J.P. Chen, W. Korsch, *Phys. Lett.* **B665**, 349 (2008) [arXiv:0803.4119 [hep-ph]].
- [35] J.M. Maldacena, *Adv. Theor. Math. Phys.* **2**, 231 (1998) [*Int. J. Theor. Phys.* **38**, 1113 (1999)] [arXiv:hep-th/9711200].
- [36] J. Polchinski, M.J. Strassler, *Phys. Rev. Lett.* **88**, 031601 (2002) [arXiv:hep-th/0109174].
- [37] A. Karch, E. Katz, D.T. Son, M.A. Stephanov, *Phys. Rev.* **D74**, 015005 (2006) [arXiv:hep-ph/0602229].

- [38] O. Andreev, V.I. Zakharov, *Phys. Rev.* **D74**, 025023 (2006) [arXiv:hep-ph/0604204].
- [39] S.D. Glazek, M. Schaden, *Phys. Lett.* **B198**, 42 (1987).
- [40] P. Hoyer, arXiv:0909.3045 [hep-ph].
- [41] N.J. Craig, D. Green, arXiv:0905.4088 [hep-ph].
- [42] J. Polchinski, M.J. Strassler, *J. High Energy Phys.* **0305**, 012 (2003) [arXiv:hep-th/0209211].
- [43] S.D. Drell, T.M. Yan, *Phys. Rev. Lett.* **24**, 181 (1970).
- [44] G.B. West, *Phys. Rev. Lett.* **24**, 1206 (1970).
- [45] S.J. Brodsky, G.F. de Teramond, *Phys. Rev. Lett.* **96**, 201601 (2006) [arXiv:hep-ph/0602252].
- [46] S.J. Brodsky, G.F. de Teramond, *Phys. Rev.* **D77**, 056007 (2008) [arXiv:0707.3859 [hep-ph]].
- [47] S.J. Brodsky, G.F. de Teramond, *Phys. Rev.* **D78**, 025032 (2008) [arXiv:0804.0452 [hep-ph]].
- [48] J. Erlich, E. Katz, D.T. Son, M.A. Stephanov, *Phys. Rev. Lett.* **95**, 261602 (2005) [arXiv:hep-ph/0501128].
- [49] L. Da Rold, A. Pomarol, *Nucl. Phys.* **B721**, 79 (2005) [arXiv:hep-ph/0501218].
- [50] S.J. Brodsky, G.F. de Teramond, *Phys. Lett.* **B582**, 211 (2004) [arXiv:hep-th/0310227].
- [51] G.F. de Teramond, S.J. Brodsky, *Phys. Rev. Lett.* **94**, 201601 (2005) [arXiv:hep-th/0501022].
- [52] S. Furui, H. Nakajima, *Phys. Rev.* **D76**, 054509 (2007) [arXiv:hep-lat/0612009].
- [53] L. von Smekal, R. Alkofer, A. Hauck, *Phys. Rev. Lett.* **79**, 3591 (1997) [arXiv:hep-ph/9705242].
- [54] A. Deur, V. Burkert, J.P. Chen, W. Korsch, *Phys. Lett.* **B650**, 244 (2007) [arXiv:hep-ph/0509113].
- [55] S.J. Brodsky, R. Shrock, *Phys. Lett.* **B666**, 95 (2008) [arXiv:0806.1535 [hep-th]].
- [56] S.J. Brodsky, H.C. Pauli, S.S. Pinsky, *Phys. Rep.* **301**, 299 (1998) [arXiv:hep-ph/9705477].
- [57] H.C. Pauli, S.J. Brodsky, *Phys. Rev.* **D32**, 2001 (1985).
- [58] S.J. Brodsky, J.R. Primack, *Ann. Phys.* **52**, 315 (1969).
- [59] S.J. Brodsky, D.S. Hwang, B.Q. Ma, I. Schmidt, *Nucl. Phys.* **B593**, 311 (2001) [arXiv:hep-th/0003082].
- [60] A. Casher, L. Susskind, *Phys. Rev.* **D9**, 436 (1974).
- [61] S.J. Brodsky, R. Shrock, arXiv:0905.1151 [hep-th], to be published in *Proc. Natl. Acad. Sci.*.
- [62] P.P. Srivastava, S.J. Brodsky, *Phys. Rev.* **D66**, 045019 (2002) [arXiv:hep-ph/0202141].

- [63] P.P. Srivastava, S.J. Brodsky, *Phys. Rev.* **D61**, 025013 (2000) [arXiv:hep-ph/9906423].
- [64] L. Motyka, A.M. Stasto, arXiv:0901.4949 [hep-ph].
- [65] S.J. Brodsky, R. Roskies, R. Suaya, *Phys. Rev.* **D8**, 4574 (1973).
- [66] O.V. Teryaev, arXiv:hep-ph/9904376.
- [67] S.J. Brodsky, C.R. Ji, *Phys. Rev.* **D33**, 2653 (1986).
- [68] K. Hornbostel, S.J. Brodsky, H.C. Pauli, *Phys. Rev.* **D41**, 3814 (1990).
- [69] S.J. Brodsky, F.J. Llanes-Estrada, J.T. Londergan, A.P. Szczepaniak, arXiv:0906.5515 [hep-ph].
- [70] G.P. Lepage, S.J. Brodsky, *Phys. Lett.* **B87**, 359 (1979).
- [71] A.V. Efremov, A.V. Radyushkin, *Phys. Lett.* **B94**, 245 (1980).
- [72] S.J. Brodsky, D.S. Hwang, *Nucl. Phys.* **B543**, 239 (1999) [arXiv:hep-ph/9806358].
- [73] S.J. Brodsky, M. Diehl, D.S. Hwang, *Nucl. Phys.* **B596**, 99 (2001) [arXiv:hep-ph/0009254].
- [74] G.P. Lepage, S.J. Brodsky, *Phys. Rev.* **D22**, 2157 (1980).
- [75] S.J. Brodsky, G.P. Lepage, SLAC-PUB-2294; Workshop on Current Topics in High Energy Physics, Cal Tech., Pasadena, Calif., Feb. 13–17, 1979.
- [76] G.F. de Teramond, S.J. Brodsky, *AIP Conf. Proc.* **1257**, 59 (2010) [arXiv:1001.5193 [hep-ph]].
- [77] Z. Abidin, C.E. Carlson, *Phys. Rev.* **D77**, 095007 (2008) [arXiv:0801.3839 [hep-ph]].
- [78] D.E. Soper, *Phys. Rev.* **D15**, 1141 (1977).
- [79] S.J. Brodsky, G.F. de Teramond, arXiv:0802.0514 [hep-ph].
- [80] P. Breitenlohner, D.Z. Freedman, *Ann. Phys.* **144**, 249 (1982).
- [81] S.J. Brodsky, G.R. Farrar, *Phys. Rev. Lett.* **31**, 1153 (1973); *Phys. Rev.* **D11**, 1309 (1975).
- [82] V.A. Matveev, R.M. Muradian, A.N. Tavkhelidze, *Lett. Nuovo Cim.* **7**, 719 (1973).
- [83] S.J. Brodsky, A.H. Mueller, *Phys. Lett.* **B206**, 685 (1988).
- [84] G. Bertsch, S.J. Brodsky, A.S. Goldhaber, J.F. Gunion, *Phys. Rev. Lett.* **47**, 297 (1981).
- [85] J.F. Gunion, S.J. Brodsky, R. Blankenbecler, *Phys. Rev.* **D8**, 287 (1973).
- [86] D.W. Sivers, S.J. Brodsky, R. Blankenbecler, *Phys. Rep.* **23**, 1 (1976).
- [87] C.G. White *et al.*, *Phys. Rev.* **D49**, 58 (1994).
- [88] R.J. Holt, *Phys. Rev.* **C41**, 2400 (1990).
- [89] C. Bochna *et al.* [E89-012 Collaboration], *Phys. Rev. Lett.* **81**, 4576 (1998) [arXiv:nucl-ex/9808001].
- [90] P. Rossi *et al.* [CLAS Collaboration], *Phys. Rev. Lett.* **94**, 012301 (2005) [arXiv:hep-ph/0405207].

- [91] S. Rock *et al.*, *Phys. Rev.* **D46**, 24 (1992).
- [92] S.J. Brodsky, B.T. Chertok, *Phys. Rev.* **D14**, 3003 (1976).
- [93] S.J. Brodsky, C.R. Ji, G.P. Lepage, *Phys. Rev. Lett.* **51**, 83 (1983).
- [94] S.J. Brodsky, G.P. Lepage, *Adv. Ser. Direct. High Energy Phys.* **5**, 93 (1989).
- [95] E.M. Aitala *et al.* [E791 Collaboration], *Phys. Rev. Lett.* **86**, 4773 (2001) [arXiv:hep-ex/0010044].
- [96] B. Clasie *et al.*, arXiv:0707.1481 [nucl-ex].
- [97] A. Airapetian *et al.* [HERMES Collaboration], *Phys. Rev. Lett.* **90**, 052501 (2003) [arXiv:hep-ex/0209072].
- [98] E.L. Berger, S.J. Brodsky, *Phys. Rev. Lett.* **42**, 940 (1979).
- [99] E.L. Berger, T. Gottschalk, D.W. Sivers, *Phys. Rev.* **D23**, 99 (1981).
- [100] E.L. Berger, S.J. Brodsky, *Phys. Rev.* **D24**, 2428 (1981).
- [101] F. Arleo *et al.*, arXiv:1006.4045 [hep-ph].
- [102] F. Arleo *et al.*, arXiv:0911.4604 [hep-ph].
- [103] S.J. Brodsky, A. Sickles, *Phys. Lett.* **B668**, 111 (2008) [arXiv:0804.4608 [hep-ph]].
- [104] V.P. Druzhinin, *PoS EPS-HEP2009*, 051 (2009) [arXiv:0909.3148 [hep-ex]] and preliminary results presented at IHCEP2010.
- [105] A.V. Radyushkin, *Phys. Rev.* **D80**, 094009 (2009) [arXiv:0906.0323 [hep-ph]].
- [106] M.V. Polyakov, *JETP Lett.* **90**, 228 (2009) [arXiv:0906.0538 [hep-ph]].
- [107] S.V. Mikhailov, N.G. Stefanis, *Mod. Phys. Lett.* **A24**, 2858 (2009) [arXiv:0910.3498 [hep-ph]].
- [108] W. Broniowski, E.R. Arriola, arXiv:1008.2317 [hep-ph].
- [109] S.J. Brodsky, G.P. Lepage, *Phys. Rev.* **D24**, 1808 (1981).
- [110] A. Danagoulian *et al.* [Hall A Collaboration], *Phys. Rev. Lett.* **98**, 152001 (2007) [arXiv:nucl-ex/0701068].
- [111] M. Diehl, T. Feldmann, R. Jakob, P. Kroll, *Eur. Phys. J.* **C8**, 409 (1999) [arXiv:hep-ph/9811253].
- [112] A. Chen, International Conference on the Structure and Interactions of the Photon and 14th International Workshop on Photon-Photon Collisions (Photon 2001), Ascona, Switzerland, 2-7 Sep., 2001.
- [113] G.R. Court *et al.*, *Phys. Rev. Lett.* **57**, 507 (1986).
- [114] I. Mardor *et al.*, *Phys. Rev. Lett.* **81**, 5085 (1998).
- [115] S.J. Brodsky, G.F. de Teramond, *Phys. Rev. Lett.* **60**, 1924 (1988).
- [116] D. Dutta, H. Gao, *Phys. Rev.* **C71**, 032201 (2005) [arXiv:hep-ph/0411267].
- [117] S.J. Brodsky, M. Karliner, *Phys. Rev. Lett.* **78**, 4682 (1997) [arXiv:hep-ph/9704379].
- [118] H.R. Grigoryan, A.V. Radyushkin, *Phys. Rev.* **D76**, 095007 (2007) [arXiv:0706.1543 [hep-ph]].

- [119] The data compilation is from M. Diehl, *Nucl. Phys. Proc. Suppl.* **161**, 49 (2006) [[arXiv:hep-ph/0510221](#)].
- [120] G. Grunberg, *Phys. Lett.* **B95**, 70 (1980); *Phys. Rev.* **D29**, 2315 (1984); *Phys. Rev.* **D40**, 680 (1989).
- [121] S.J. Brodsky, H.J. Lu, *Phys. Rev.* **D51**, 3652 (1995) [[arXiv:hep-ph/9405218](#)]; S.J. Brodsky, G.T. Gabadadze, A.L. Kataev, H.J. Lu, *Phys. Lett.* **B372**, 133 (1996) [[arXiv:hep-ph/9512367](#)].
- [122] T. Appelquist, M. Dine, I.J. Muzinich, *Phys. Lett.* **B69**, 231 (1977).
- [123] J.D. Bjorken, *Phys. Rev.* **148**, 1467 (1966).
- [124] A. Deur, [arXiv:0907.3385](#) [[nucl-ex](#)].
- [125] S.J. Brodsky, G.F. de Teramond, A. Deur, *Phys. Rev.* **D81**, 096010 (2010) [[arXiv:1002.3948](#) [[hep-ph](#)]].
- [126] J.M. Cornwall, *Phys. Rev.* **D26**, 1453 (1982).
- [127] A.C. Aguilar *et al.*, *Phys. Rev.* **D80**, 085018 (2009) [[arXiv:0906.2633](#) [[hep-ph](#)]].
- [128] S.D. Drell, A.C. Hearn, *Phys. Rev. Lett.* **16**, 908 (1966); S.B. Gerasimov, *Sov. J. Nucl. Phys.* **2** 430 (1966) [*Yad. Fiz.* **2**, 598 (1966)].
- [129] H. Gao, L. Zhu, *AIP Conf. Proc.* **747**, 179 (2005) [[arXiv:nucl-ex/0411014](#)].
- [130] J.C.R. Bloch, *Phys. Rev.* **D66**, 034032 (2002) [[arXiv:hep-ph/0202073](#)]; P. Maris, P.C. Tandy, *Phys. Rev.* **C60**, 055214 (1999) [[arXiv:nucl-th/9905056](#)]; C.S. Fischer, R. Alkofer, *Phys. Lett.* **B536**, 177 (2002) [[arXiv:hep-ph/0202202](#)]; C.S. Fischer, R. Alkofer, H. Reinhardt, *Phys. Rev.* **D65**, 094008 (2002) [[arXiv:hep-ph/0202195](#)]; R. Alkofer, C.S. Fischer, L. von Smekal, *Acta Phys. Slov.* **52**, 191 (2002) [[arXiv:hep-ph/0205125](#)]; M.S. Bhagwat, M.A. Pichowsky, C.D. Roberts, P.C. Tandy, *Phys. Rev.* **C68**, 015203 (2003) [[arXiv:nucl-th/0304003](#)].
- [131] V.D. Burkert, B.L. Ioffe, *Phys. Lett.* **B296**, 223 (1992); *J. Exp. Theor. Phys.* **78**, 619 (1994) [*Zh. Eksp. Teor. Fiz.* **105**, 1153 (1994)].
- [132] G. Parisi, *Phys. Lett.* **B39**, 643 (1972).
- [133] S.J. Brodsky, R. Shrock, [arXiv:0803.2541](#) [[hep-th](#)].
- [134] S.J. Brodsky, R. Shrock, [arXiv:0803.2554](#) [[hep-th](#)].
- [135] K. Langfeld *et al.*, *Phys. Rev.* **C67**, 065206 (2003).
- [136] K.D. Lane, *Phys. Rev.* **D10**, 2605 (1974).
- [137] H.D. Politzer, *Nucl. Phys.* **B117**, 397 (1976).
- [138] T. Banks, A. Casher, *Nucl. Phys.* **B169**, 103 (1980).
- [139] M. Karliner, *Nucl. Phys. Proc. Suppl.* **187**, 21 (2009) [[arXiv:0806.4951](#) [[hep-ph](#)]].
- [140] A. Chodos, C.B. Thorn, *Phys. Rev.* **D12**, 2733 (1975).
- [141] G.E. Brown, M. Rho, *Phys. Lett.* **B82**, 177 (1979).
- [142] A. Hosaka, H. Toki, *Phys. Rep.* **277**, 65 (1996).
- [143] S.J. Brodsky, D.S. Hwang, I. Schmidt, *Phys. Lett.* **B530**, 99 (2002) [[arXiv:hep-ph/0201296](#)].

- [144] J.C. Collins, *Phys. Lett.* **B536**, 43 (2002) [arXiv:hep-ph/0204004].
- [145] D. Boer, S.J. Brodsky, D.S. Hwang, *Phys. Rev.* **D67**, 054003 (2003) [arXiv:hep-ph/0211110].
- [146] S.J. Brodsky, A.H. Hoang, J.H. Kuhn, T. Teubner, *Phys. Lett.* **B359**, 355 (1995) [arXiv:hep-ph/9508274].
- [147] J. Collins, J.W. Qiu, *Phys. Rev.* **D75**, 114014 (2007) [arXiv:0705.2141 [hep-ph]].
- [148] P. Maris, C.D. Roberts, P.C. Tandy, *Phys. Lett.* **B420**, 267 (1998) [arXiv:nucl-th/9707003].
- [149] P. Maris, C.D. Roberts, *Phys. Rev.* **C56**, 3369 (1997) [arXiv:nucl-th/9708029].
- [150] B.L. Ioffe, K.N. Zyablyuk, *Eur. Phys. J.* **C27**, 229 (2003) [arXiv:hep-ph/0207183].
- [151] M. Davier, A. Hocker, Z. Zhang, *Nucl. Phys. Proc. Suppl.* **169**, 22 (2007) [arXiv:hep-ph/0701170].
- [152] M. Davier *et al.*, *Eur. Phys. J.* **C56**, 305 (2008) [arXiv:0803.0979 [hep-ph]].

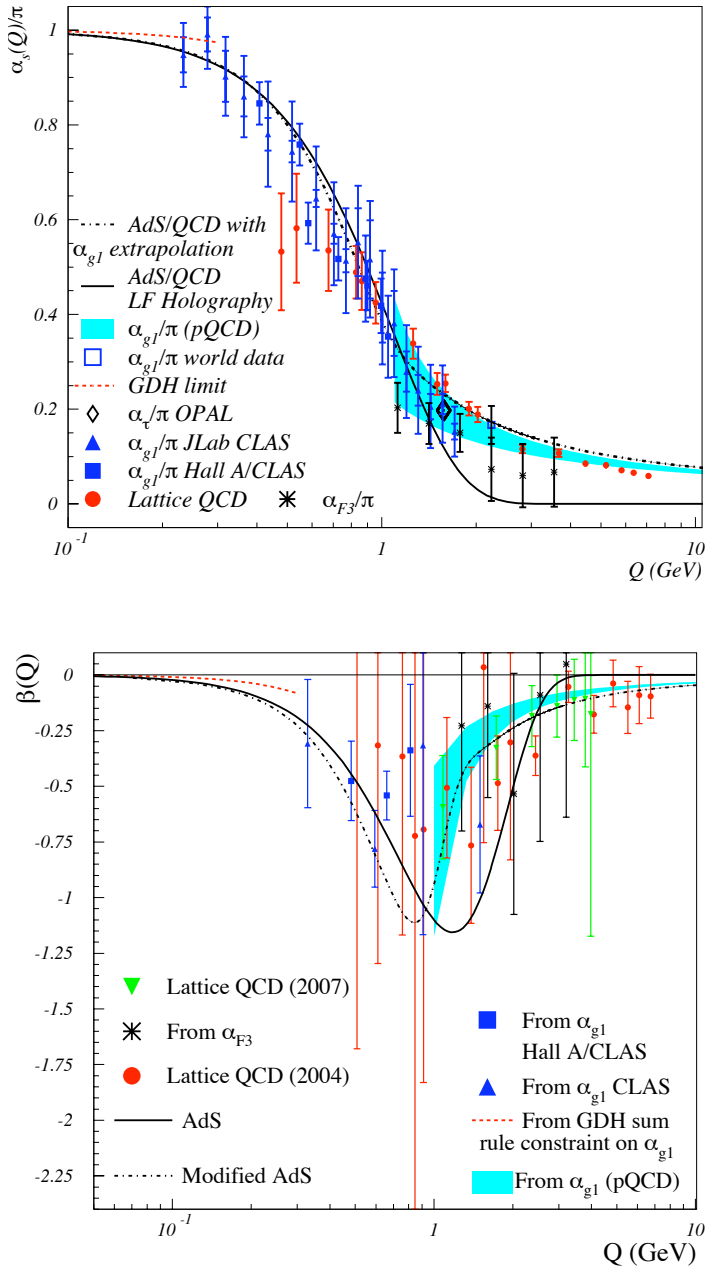


Fig. 7. (Top) Effective coupling from LF holography for $\kappa = 0.54$ GeV compared with effective QCD couplings extracted from different observables and lattice results. (Bottom) Prediction for the β -function compared to lattice simulations, JLab and CCFR results for the Bjorken sum rule effective charge.